AJUR

American Journal of
Undergraduate Research

Volume 14 | Issue 4 | March 2018

www.ajuronline.org

Print Edition ISSN 1536-4585
Online Edition ISSN 2375-8732

AJUR
American Journal of
Undergraduate Research

Volume 14 | Issue 4 | March 2018 *www.ajuronline.org*

American Journal of Undergraduate Research (AJUR) is a national, peer-reviewed, open-source, quarterly, multidisciplinary student research journal. It is indexed internationally by EBSCO, and is listed via the Library of Congress under ISSNs of 1536-4585 (for print) and 2375-8732 (for web). The journal was established in 2002.

EDITORIAL TEAM *Volume 14 | Issue 4 | March 2018*

EDITORIAL BOARD *by subject area*

SPECIAL THANKS

AJUR is made possible through the assistance of our sponsors.

Support for this issue has been provided by the Office of the Provost at the State University of New York at Oswego. Thank you!

Thermodynamics of *Concanavalin A* Self-Association in the Presence of Osmolytes

Tyler Pfister, Shamus Cooper, & Jeffrey K. Myers*

Department of Chemistry, Davidson College, NC

Students: Typfister17@alumni.davidson.edu, Shcooper16@alumni.davidson.edu*
Mentor: Jemyers@davidson.edu

ABSTRACT
Protein-protein interactions are critical for biological function and depend significantly on environmental factors. A wide variety of small organic molecules that comprise the cellular environment are capable of interacting with proteins to affect folding, binding, and association. The plant lectin concanavalin A (ConA) undergoes a reversible, pH dependent dimer-to-tetramer equilibrium and has been used in our laboratory as a model system to study the effect of osmolytes on protein self-association. Previous research determined that trimethylamine *N*-oxide (TMAO) stabilizes the tetrameric conformation, while urea favors the dimer. Studying the equilibrium over a range of temperatures allowed quantification of the enthalpy change (ΔH) and entropy change (ΔS) of tetramer formation. Urea increased both the ΔH and ΔS of tetramer formation, while TMAO decreased both. These effects are consistent with preferential hydration of the dimer-dimer interface in TMAO solution and preferential binding of urea to the interface.

KEYWORDS
Concanavalin A; Osmolytes; Trimethylamine *N*-oxide; Urea; Protein-Protein Interaction; Equilibrium; Enthalpy; Preferential Hydration

INTRODUCTION

Many proteins in biological contexts are known to exist as oligomers; therefore it is necessary to study the process of protein self association to gain a full picture of protein folding. The conformational changes involved in protein folding are sensitive to environmental conditions including pH, temperature, and possible interactions with small molecules. Osmolytes are a class of small organic molecules that accumulate naturally in cells where they function to mitigate osmotic stress.[1] Osmolytes have been characterized in detail with respect to their ability to alter the thermodynamics of monomeric protein folding.[2 – 7] However, relatively few studies have addressed the effect of osmolytes on protein-protein interactions.[8 – 10]

Most osmolytes stabilize protein structure, and are thought to be preferentially excluded from the peptide backbone, causing the protein to favor a folded state where there is less surface area to interact with the osmolyte.[4, 5, 11, 12] Additionally, osmolytes are able to sequester water molecules, resulting in a local hydrophobic environment that favors the folded protein. Consequently, the melting temperature (T_m) and the free energy of unfolding (ΔG) are elevated in the presence of stabilizing osmoltyes.[4, 11] Evidence also supports osmolytes' role in structuring regions of proteins that are intrinsically disordered. This may allow for molecular recognition and ligand binding when these regions are stabilized in correct conformations. It has been suggested that diseases like Alzheimer's and Parkinson's that involve formation of amyloid fibrils might result in part from osmolyte stabilization of certain oligomeric precursors.[12]

Destabilizing osmolytes are thought to interact favorably with the peptide backbone through hydrogen bonding, thus favoring unfolding. Destabilizing osmolytes pose their own threat to protein function since moderate concentrations of compounds like urea (which accumulates in cartilaginous fish)[13, 14] lead to destabilization of proteins. Lin *et al.* found that trimethylamine *N*-oxide (TMAO), a stabilizing osmolyte, can help combat the denaturation effects of urea. They determined that urea preferentially bound to the denatured form of the protein, while TMAO was preferentially excluded. This results in a change in the ΔG; urea decreases the ΔG resulting in a smaller T_m. TMAO increased ΔG, resulting in a larger T_m. In combination, the net effect was the algebraic sum of their individual effects.[13] Wang and Bolen reached a similar conclusion by using a transfer model to measure the transfer free energy change of proteins and individual amino acids.[14] This allowed them to quantify the transfer free energy of the side chains of each amino acid. From their results, it was concluded that TMAO preferentially interacts with the backbone to destabilize the denatured state. Mello and Barrick, who showed that free energy transitions varied linearly with TMAO concentration, further validated these results.[15]

Despite the prevalence of research concerning the influence of osmolytes on protein denaturation, there is considerably less research on their effect on protein-protein interactions. The binding of protein monomers to each other is an inherent part of the folding of oligomeric proteins, and can be viewed as a special case of a macromolecule binding to its ligand. The ability of osmolytes to preferentially interact with water or protein may have an effect on the change in free energy of binding.[16] This effect is due in part to a hydration effect and not the result of crowding. When the binding of a TATA-box binding protein to its 20 bp DNA promoter was examined with betaine, sucrose, and triethylene glycol (TEG), there was no change in the dissociation constant (K_d) in the presence of TEG, but betaine and sucrose decreased the K_d 18 and 5-fold respectively. This results from the increased number of water molecules released upon binding and concomitant entropy change.[16, 17] Alternately, osmolytes can decrease the binding affinity through increased water uptake used to mediate the ligand binding. One example is the binding of lysozyme to a monoclonal antibody, which shows a 26-fold binding affinity decrease in the presence of betaine.[18] Additionally, osmolytes can preferentially interact with ligands to change the free energy of binding.[16]

Previous work in our laboratory has established Concanavalin A (ConA) as a convenient model system in which to study the effects of osmolytes on protein self-association.[10] Concanavalin A is a commercially available plant lectin from jack bean, *Canavalia ensiformis*. Its chemical and physical properties have been extensively characterized in earlier works.[19, 20] ConA is a metalloprotein that binds α-D-mannopyranoside and β-D-glucopyranoside through the use of one manganese (Mn^{2+}) and one calcium (Ca^{2+}) per subunit.[21 – 25] This unique functionality has lead to its use in analytical separation of glycosylated proteins and mitogen stimulation of the immune system. The secondary structure of the protein consists of two large anti-parallel β-sheets. A twisted sheet of seven strands passes through the center and the back is formed by a bowed six-strand sheet.[21 – 23] ConA can be found as a tetramer or dimer under cellular conditions, however the tetramer predominates at neutral pH. The structure can be described as a dimer of dimers with a center water-filled cavity and a relatively large interface, the surface area of which is estimated to be 1150 $Å^2$ per dimer.[10] The equilibrium has been studied previously using sedimentation equilibrium in Senear and Teller. They determined that protonation of a single Histidine residue at pH 6.55, likely His 51 or His 121, leads to destabilization of the tetramer.[26]

ConA is a convenient model because it allows for study of the equilibrium by titrating samples to change the pH and monitoring the reversible dimer to tetramer process through circular dichroism (CD). Near UV CD proved useful in monitoring the equilibrium due to small changes in the environment surrounding aromatic side chains upon tetramer formation. It was found that osmolytes that are known to stabilize monomeric protein folding also favor formation of the ConA tetramer. Urea, a destabilizing osmolyte, favored the dimeric form of ConA. However, theoretical models did not reliably predict the effects of osmolytes on ConA association in a quantitative fashion. Thus, further research is needed to fully understand the details of osmolyte interactions with proteins.

In this work, the temperature dependence of ConA association in the presence of TMAO and urea was analyzed to determine the effect of these osmolytes on the enthalpy and entropy changes that accompany association.

METHODS AND PROCEDURES

ConA preparation.

ConA, lyophilized from *Canavalia ensiformis* (jack bean), was purchased from Sigma and found to contain a significant amount of hydrolyzed subunits. Purification was described previously [10, 26] and proceeded by preparing a 10 mg/mL solution of ConA in 5 mM sodium acetate buffer (pH = 2.3), which was then dialyzed against 1% ammonium bicarbonate (pH = 7.0) for 10-12 hours at 37ºC. Dialysis was followed by centrifugation at 25,000 g for 20 minutes to remove precipitate. The supernatant was passed through a 0.22 μm filter and dialyzed against ConA storage buffer (50 mM sodium phosphate pH 6.5, 0.5 M NaCl, 0.2 mM $CaCl_2$ and $MnCl_2$, 0.1 mM NaN_3). Protein concentration was determined using UV absorbance spectroscopy at 280 nm using an extinction coefficient $E_{cm}^{1\%}$=11.4.[26]

Spectroscopic measurements of equilibrium

All near-UV CD measurements were obtained on a Jasco J-815 spectropolarimeter using a 1.0 cm path length quartz cuvette with a bandwidth of 2.0 nm while temperature was maintained using a Peltier-type temperature controller (Quantum Northwest) under constant stirring.

Samples were prepared with 0.5 mg/mL ConA in titration buffer with or without 1.0 M osmolytes. Titration buffer was made 5 times concentrated (250 mM acetate, 250 mM phosphate, 0.5 M NaCl, pH = 7.5). TMAO was prepared at 4.0 M in deionized water and washed with amberlite to remove contaminants. The resin was filtered away and concentration was determined using refractive index measurement. Urea was prepared at 6 M in deionized water and the concentration was again determined by refractive index measurement. Samples were titrated from high pH to low with 6.05 M HCl using variable volumes while stirring. Separate titrations were conducted at different temperatures between 15-35ºC using 5ºC increments. At each pH point, CD signal

was determined by taking the average of 30 two-second measurements at a wavelength of 284.0 nm and bandwidth of 2.0 nm. Signals were corrected to account for dilution caused by adding HCl solution. The pH at each point was determined previously by a mock titration that used ConA storage buffer without protein mixed with titration buffer.

Data analysis.
The following equation was fit to the data from each titration:

$$Signal = \frac{[m_l \times pH + b_l] + [m_u \times pH + b_u]}{1 + 10^{[n(pH - pH_{mid})]}} \quad \textbf{Equation 1.}$$

where m_l and m_u are the slopes of the lower and upper baselines respectively, b_l and b_u are the intercepts of the lower and upper baselines respectively, n is the number of protons dissociated per dimer, and pH_{mid} is the observed pH midpoint of transition. Senear and Teller previously determined that the equilibrium can be described using the following equation:[26]

$$\ln K_{app} = \ln K_{assoc} - 4 \ln (1 + 10^{-pH} / 10^{-pK_a}) \quad \textbf{Equation 2.}$$

where K_{app} is the apparent association constant, K_{assoc} is the association constant for deprotonated dimers and the pK_a of the relevant histidine residue was determined to be 6.55 by Senear and Teller.[26] K_{app} was determined to be 1.11 x 10^5 at the midpoint of the pH transition for the constant 0.50 mg/mL ConA concentration used. Van't Hoff plots were then constructed and the ΔH and ΔS were determined from the slopes of fitted lines.

RESULTS

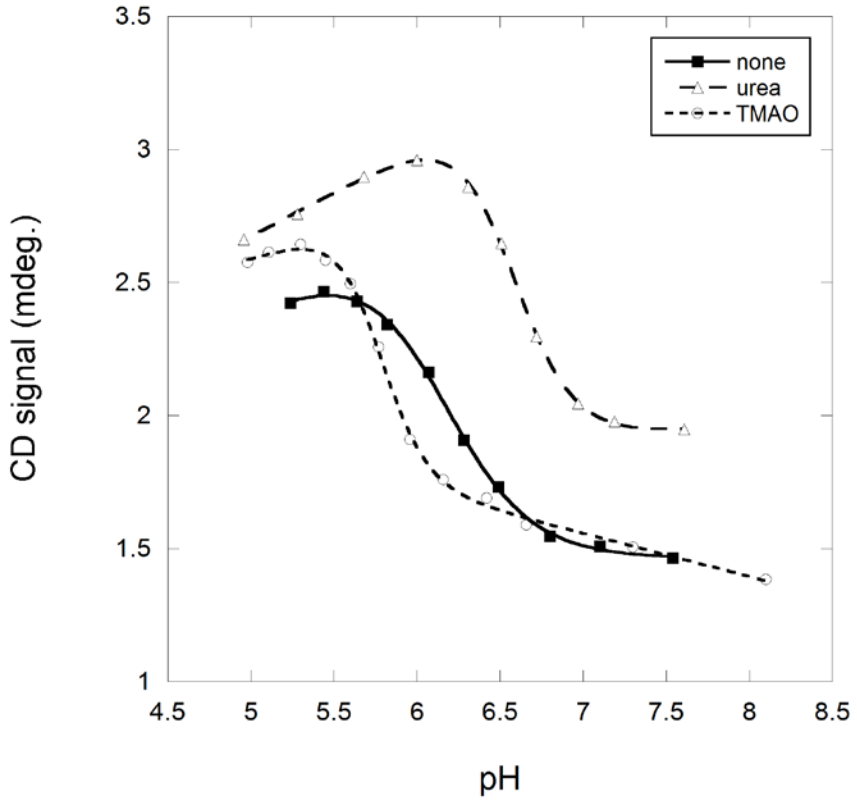

Figure 1. Titrations followed by circular dichroism. pH induced transitions from tetramer (neutral pH) to dimer (acidic pH) of ConA at 20°C followed by circular dichroism spectroscopy. Lines are fits to **Equation 1**, used to determine the pH midpoint.

Data from representative titrations are shown in **Figure 1**. The tetramer-to-dimer transition occurs when samples were titrated to low pH from a starting pH around 7.5. The initial and final baselines appear similar for titrations containing no osmolyte compared with those containing TMAO. This is not the case when ConA was titrated from pH 7.5 to 5.0 in 1.0 M urea **Figure 1**. The addition of urea appears to affect the structure of the tetramer as evidenced by the change in high pH baseline. This is possibly due to destabilization of protein structure. An analogous effect is observed in the low pH baseline. Also notable is the fact that TMAO binds a proton with a pKa of 4.7, so that at the lower pH range of our experiments some of the TMAO is protonated; protonated TMAO might affect the equilibrium differently.[27]

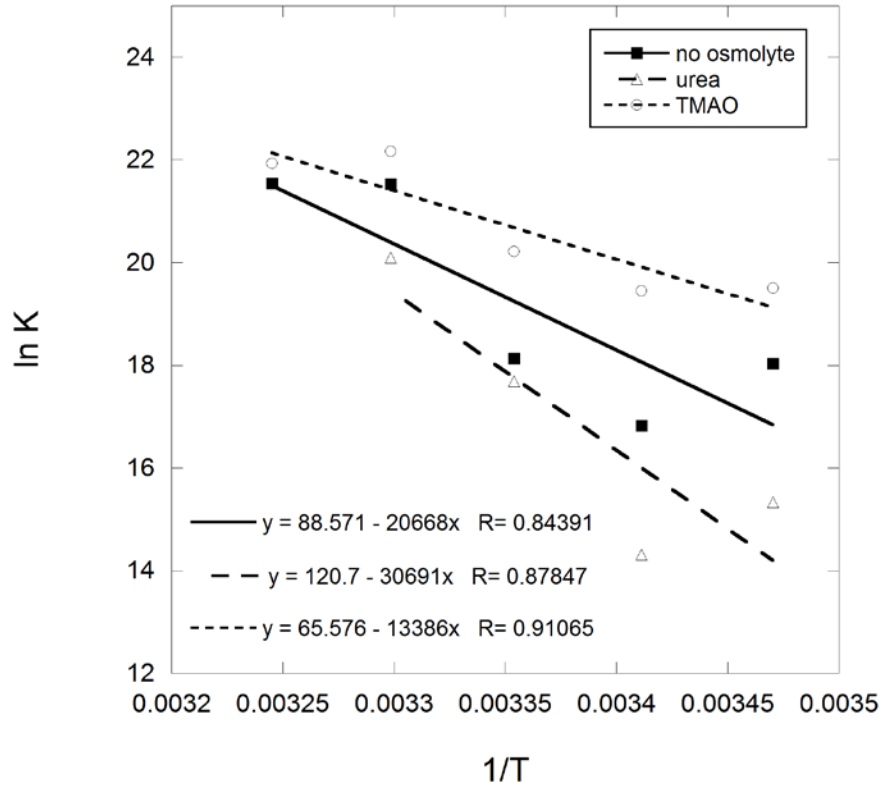

Figure 2. Van't Hoff plots for ConA association with TMAO, urea, and in the absence of osmolytes. Association constants were calculated using pH midpoint data from titrations at varying temperatures. Equations for linear fits are shown.

Osmolyte	ΔG_{298} (kJ/mol)	ΔH_{298} (kJ/mol)	ΔS_{298} (J/mol·K)
None	-44.9±0.8	171±63	736±211
Urea	-41.9±0.8	255±98	1003±332
TMAO	-50.3±0.8	111±29	545±98

Table 1. Thermodynamic Data for ConA Association. Quantities for ΔH and ΔS (± s.e) were determined from the lines of best fit in **Figure 2**. Free energy changes were calculated from ΔG = ΔH – TΔS, and the error was assumed identical to Silvers and Myers (2013).[10]

In all cases, a sigmoidal shaped curve was obtained; these curves were fit to **Equation 1** to provide the midpoint pH values. At these pH values, half the ConA subunits exist in dimers, half in tetramers. The change in tetramer stability caused by osmolytes is qualitatively evident in the shifting of the pH midpoint. The increase in the pH midpoint of urea signals that the tetramer becomes unstable at a much higher pH, thus the dimer is favored in the presence of urea. Conversely, the decrease in pH midpoint upon adding TMAO signals that the tetramer is stabilized at lower pH. These results confirm the observation noted by Silvers and Myers that osmolytes can stabilize and destabilize not only protein secondary and tertiary structure but also quaternary structure.[10] From this data, association constant values were calculated from **Equation 2**[26] and used to construct the Van't Hoff plots shown in **Figure 2**. From the data in **Figure 2**, the free energy change, enthalpy change, and entropy change for the association of two dimers into a tetramer were determined, **Table 1**. The association is endothermic and driven by entropy, as has been found previously.[26, 28] Without osmolytes, tetramers were present at higher temperatures (≥40ºC) over the pH range of 4.0 to 7.5 with little dissociation as recorded by CD measurements, while only dimeric ConA was present at low temperatures, despite pH changes.

DISCUSSION

Urea clearly increased both ΔH and ΔS, while TMAO decreased both, **Table 1**. These changes can be interpreted by considering the effect of the osmolytes on the hydration of the dimer-dimer interface. There are two main contributors to the ΔH of association. One, a negative contribution from the new interactions formed between the subunits. Two, a positive contribution from the interactions broken between the protein and the water—and other solutes—that were occupying the surface of the interface. Likewise, there are two main contributors to the ΔS of association. One, a negative contribution from the organization of multiple subunits into a smaller number of oligomers and the fixing of side chains in the interface. Two, a positive contribution caused by the release of water—and other solutes—from the interface region. In the case of ConA, the solvent contribution to both ΔH and ΔS predominates. The association of the dimers is thus driven by the release of water from the interface region. Given the known effect of osmolytes on protein hydration, the alteration of thermodynamic parameters is not unexpected.

The change in enthalpy can be explained by considering the influence of urea and TMAO on the hydration of the dimer-dimer interface. It was suggested in Senear and Teller that the large and positive enthalpy of association was due to the steric hindrance around the Gln-122 residue, which is disordered in the tetramer.[26] This appears less likely because of the impossibility of interaction of urea with the backbone of the residue that was stated as a mechanism for how urea destabilizes protein structure in Street *et al*.[29] Instead, an alternate picture proposed by Huet and Claverie suggested that in the association of two dimers, the water associated with the hydrophobic binding region would require energy to displace the hydrogen bonds from the protein surface to bond with the bulk solvent.[28] This model appears much more attractive as it allows for incorporation of the preferential hydration hypothesis. The molecular picture explains that when water transitions from bonding with the binding region to the bulk solvent, the change in bond energies results in the enthalpy. TMAO is preferentially excluded from the molecular surface, so water will accumulate around the protein under high concentrations of TMAO. A water mediated effect on enthalpy was also suggested in a study that found that there was no difference in enthalpy associated with TMAO stabilization of poly-alanine or poly-leucine chains.[30] In comparison, urea will bind to the protein preferentially, mainly by hydrogen bonding to the peptide backbone, so its removal to the water poses a larger cost in enthalpy. A synthesis of the two competing theories could be a two stage model of protein-self assembly, similar to the model Chong and Ham proposed for β-amyloid formation in Alzheimer's.[31] The initial, long-range attraction is mediated by the enthalpy driven hydration force of hydrophilic residues. After initial interaction, a short-range entropic force drives the association to completion by de-solvating the contact surfaces. This might explain the fact that urea increases the enthalpy change since more energy would be required to break the initial bond between the hydrophilic residue and urea, while still explaining the decreased enthalpy change seen in the TMAO results.

The preferential hydration model of osmolytes can similarly account for the change in entropy, **Table 1**. Urea, due to its tendency to interact with the protein backbone, localizes to the surface. Urea was theorized to act as a buffer that mitigates the entropic cost of exposing hydrophobic residues.[3] This would enhance the stability of the dimer and the exposed hydrophobic dimer-dimer contact, reducing the need for water molecules to organize themselves to solvate the exposed interface. Conversely, TMAO is preferentially excluded from the protein surface and solvation of the dimer-dimer surface constitutes a larger entropic cost than solvation in the trials without osmolyte.[5] Essentially, the alteration of ΔS can be attributed to the relative increase in water ordering that occurs upon dissociation in TMAO and the relative decrease in water ordering that occurs upon dissociation in urea.

Valuable information may also be gained from examination of heat capacity change (ΔC_p). Although Senear and Teller were able to determine a value of -800 cal/mol•K, our data was collected, by necessity, over a fairly narrow temperature range, and attempts to accurately fit for ΔC_p were unsuccessful. A positive ΔC_p is common for protein unfolding according to Prabhu and Sharp,[32]

thus a negative value for self-association would be expected. The hydration of the protein is the major contributor to ΔC_p, [32, 33] thus a large variation upon addition of osmolytes would be expected since osmolytes change the water's interaction with the protein. It is anticipated that future work will address the effect of osmolytes on the heat capacity change of association.

CONCLUSIONS

The introduction of osmolytes like urea and TMAO causes a change in the association constant due to an increase in ΔH and ΔS in the presence of urea and a decrease in the presence of TMAO. Our results are consistent with preferential hydration in TMAO solutions and preferential binding to urea in urea solutions. Previously, osmolytes were almost exclusively studied in the context of protein folding and not protein-protein interactions. To gain a more complete understanding of proteins in a biological context, where many form oligomers, it is necessary to understand how osmolytes influence the thermodynamics of protein protein interactions. While pH, temperature, and salt ions are classically thought of as key environmental factors influencing protein binding, osmolytes may also have important effects on the thermodynamic parameters of protein-protein and protein ligand interactions.

ACKNOWLEDGEMENTS

The authors thank Connor Evins for carrying out some preliminary experiments, Lee Maiorano for technical assistance, and Davidson College for financial support of this research.

REFERENCES

1. Yancey, P. H., Clark, M. E., Hand, S. C., Bowlus, R. D., and Somero, G. N. (1982) Living with water stress: Evolution of osmolyte systems, *Science* 217, 1214−1222. DOI: 10.1126/science.7112124
2. Timasheff, S. N. (2001) Protein-solvent preferential interactions, protein hydration, and the modulation of biochemical reactions by solvent components, *Proc Natl Acad Sci* 99, 9721 – 9726. DOI: 10.1073/pnas.122225399
3. Adamczak, B., Wieczór, M., Kogut, M., Stangret, J., and Czub, J. (2016) Molecular basis of the osmolyte effect on protein stability: a lesson from the mechanical unfolding of lysozyme, *Biochem J* 473, 1 – 25. DOI: 10.1042/BCJ20160604
4. Schellman, J. A. (2003) Protein stability in mixed solvents: a balance of contact interaction and excluded volume, *Biophys J* 85, 108 – 125. DOI: 10.1016/S0006-3495(03)74459-2
5. Courtenay, E. S., Capp, M. W., Anderson, C. F., and Record, M. T., Jr. (2000) Vapor pressure osmometry studies of osmolyte−protein interactions: implications for the action of osmoprotectants in vivo and for the interpretation of "osmotic stress" experiments in vitro, *Biochemistry* 39, 4455 – 4471. DOI: 10.1021/bi992887l
6. Guinn, E. J., Pegram, L. M., Capp, M. W., Pollock, M. N., and Record, M. T., Jr. (2011) Quantifying why urea is a protein denaturant, whereas glycine betaine is a protein stabilizer. *Proc Natl Acad Sci* USA 108, 16932 – 16937. DOI: 10.1073/pnas.1109372108
7. Diehl, R. C., Guinn, E. J., Capp, M. W., Tsodikov, O. V., and Record, M. T., Jr. (2013) Quantifying additive interactions of the osmolyte proline with individual functional groups of proteins: comparisons with urea and glycine betaine, interpretation of m-values, *Biochemistry* 52, 5997 – 6010. DOI: 10.1021/bi400683y
8. Patel, C. N., Noble, S. M., Weatherly, G. T., Tripathy, A., Winzor, D. J., and Pielak, G. J. (2002) Effects of molecular crowding by saccharides on α-chymotrypsin dimerization, *Protein Sci* 11, 997 – 1003. DOI: 10.1110/ps.4450102
9. Chebotareva, N. A., Andreeva, I.E., Makeeva, V. F., Livanova, N. B., and Kurganov, B. I. (2004) Effect of molecular crowding on self-association of phosphorylase kinase and its interaction with phosphorylase b and glycogen, *J Mol Recognit* 17, 426 – 432. DOI: 10.1002/jmr.696
10. Silvers, T. R., and Myers, J. K. (2013). Osmolyte effects on the self-association of concanavalin A: Testing theoretical models, *Biochemistry* 52, 9367 – 9374. DOI: 10.1021/bi401049s
11. Arakawa, T., and Timasheff, S. N. (1985) The stabilization of proteins by osmolytes, *Biophys J* 47, 411 – 414. DOI: 10.1016/S0006-3495(85)83932-1
12. Khan, S. H., Ahmad, N., Ahmad, F., and Kumar, R. (2010) Naturally occurring organic osmolytes: From cell physiology to disease prevention, *IUBMB Life* 62, 891 – 895. DOI: 10.1002/iub.406
13. Lin, T. Y., and Timasheff, A. N. (1994) Why do some organisms use a urea-methylamine mixture as osmolyte? Thermodynamic compensation of urea and trimethylamine N-oxide interactions with protein, *Biochemistry* 33, 12695 – 12701. DOI: 10.1021/bi00208a021
14. Wang, A., Bolen, D. W. (1997) A naturally occurring protective system in urea-rich cells: Mechanism of osmolyte protection of proteins against urea denaturation, *Biochemistry* 36, 9101 – 9108. DOI: 10.1021/bi970247h

15. Mello, C., and Barrick, D. (2003) Measuring the stability of partly folded proteins using TMAO, *Protein Sci* 12, 1522 – 1529. DOI: 10.1110/ps.0372903

16. Duff, M. R., and Howell, E. E. (2015) Thermodynamics and solvent linkage of macromolecule–ligand interactions, *Methods* 76, 51 – 60. DOI: 10.1016/j.ymeth.2014.11.009

17. Bergqvist, S., O'Brien, R., and Ladbury, J. E. (2001). Site-specific cation binding mediates TATA binding protein − DNA interaction from a hyperthermophilic archaeon, *Biochemistry 40*, 2419 – 2425. DOI: 10.1021/bi002488m

18. Xavier, K. A., Shick, K. A., Smith-Gil, S. J., and Willson, R. C. (1997) Involvement of water molecules in the association of monoclonal antibody HyHEL-5 with bobwhite quail lysozyme, *Biophys J* 73, 2116 – 2125. DOI: 10.1016/S00063495(97)78242-0

19. Olson, M. O. J., and Liener, I. E. (1967) Some physical and chemical properties of concanavalin a phytohemagglutinin of jack bean, *Biochemistry* 6, 105 – 111. DOI: 10.1021/bi00853a018

20. Agrawal, B. B., and Goldstein, I. J. (1968) Protein-carbohydrate interaction. VII. Physical and chemical studies on concanavalin A, the hemagglutinin of the jack bean, *Arch Biochem Biophys* 124, 218 – 229. DOI: 10.1016/0003-9861(68)903226

21. Hardman, K. D., and Ainswort, C. F. (1972) Structure of concanavalin A at 2.4 angstrom resolution, *Biochemistry* 11, 4910 – 4919. DOI: 10.1021/bi00776a006

22. Becker, J. W., Reeke, G. N., Jr, Wang, J. L., Cunningham, B. A., and Edelman, G. M. (1975) The covalent and three-dimensional structure of concanavalin A. III. Structure of the monomer and its interactions with metals and saccharides, *J Biol Chem* 250, 1513 – 1524.

23. Parkin, S., Rupp, B., and Hope, H. (1996) Atomic resolution structure of concanavalin A at 120 K, *Acta Crystallogr, Sect D: Biol Crystallogr* 52, 1161 – 1168. DOI: 10.1107/S0907444996009237

24. Brewer, C. F., Marcus, D. M., and Grollman, A. P. (1974) Interactions of saccharides with concanavalin: a relation between calcium ions and the binding of saccharides to concanavalin A, *J Biol Chem* 249, 4614 – 4616. DOI: 10.1021/bi00746a023

25. Goldstein, I. J., and Poretz, R. D. (1971) Protein-carbohydrate interaction: On the mode of binding of aromatic moieties to concanavalin A, *Biochem Pharmacol* 20, 2727 – 2739. DOI: 10.1016/0006-2952(71)90182-1

26. Senear, D. F., and Teller, D. C. (1981) Thermodynamics of concanavalin A dimer-tetramer self-association: sedimentation equilibrium studies, *Biochemistry* 20, 3076 – 3083. DOI: 10.1021/bi00514a014

27. Singh, R., Haque, I., and Ahmad, F. (2005) Counteracting osmolyte trimethylamine *N*-oxide destabilizes proteins at pH below its pK_a: Measurements of thermodynamic parameters of proteins in the presence and absence of trimethylamine *N*-oxide, *J Biol Chem* 280, 11035 – 11042. DOI: 10.1074/jbc.M410716200

28. Huet, M., Claverie, J. M. (1978) Sedimentation studies of the reversible dimer-tetramer transition kinetics of concanavalin A, *Biochemistry* 17, 236 – 241. DOI: 10.1021/bi00595a007

29. Street, T. O.; Bolen, D. W.; Rose, G. D. (2006) A molecular mechanism for osmolyte-induced protein stability. *Proc Natl Acad Sci* 103, 13997 – 14002. DOI: 10.1073/pnas.0606236103

30. Su, Z., Srinivasa, J. R., and Dias, C. L. (2015) Roles of urea and TMAO on the interaction between extended non-polar peptides, *Biophys J* 108, 519 – 520. DOI: 10.1016/j.bpj.2014.11.2849

31. Chong, S. H., and Ham, S. (2012) Impact of chemical heterogeneity on protein self-assembly in water, *Proc Acad Natl Sci* 109, 7636 – 7641. DOI: 10.1073/pnas.1120646109

32. Prabhu, N. V., Sharp, K. A. (2005) Heat capacity in proteins, *Annu Rev Phys Chem* 56, 521 – 548. DOI: 10.1146/annurev.physchem.56.092503.141202

33. Sturtevant, J. M. (1977) Heat capacity and entropy changes in processes involving proteins, *Proc Acad Natl Sci* 74, 22362240.

ABOUT THE STUDENT AUTHORS

Tyler Pfister graduated from Davidson College in 2017 with a degree in chemistry and emphasis in biological chemistry. He is now a research fellow at the National Institute of Health and plans to pursue a MD/PhD. Shamus Cooper graduated from Davidson College in 2016 with a degree in chemistry and emphasis in biological chemistry. He will be applying to dental programs.

PRESS SUMMARY

To understand how proteins interact with each other in cells, we studied how proteins separate in the presence of osmolytes. These small organic compounds are produced in many different organisms, where they help to mitigate water stress. We found that it takes less energy to separate proteins when urea, an osmolyte filtered out of your body into urine, is included. Conversely, TMAO, an osmolyte found in fish, causes an increase in the energy required to separate proteins. These results will help us understand how the cellular environment can influence the interactions of proteins with each other, a process that is fundamental in the progression of several neurodegenerative diseases like Alzheimer's and Parkinson's Disease.

Perception of peer drinking and access to alcohol mediate the effect of residence status on alcohol consumption

Katrina A. Williams[a], Nathaniel S. Thomas*[b,c], Amy E. Adkins[b,c], & Danielle M. Dick[b,c,d]*

[a] *Department of Kinesiology and Health Sciences, Virginia Commonwealth University, Richmond, VA, United States*
[b] *College Behavioral and Emotional Health Institute, Virginia Commonwealth University, Richmond, VA, United States*
[c] *Department of Psychology, Virginia Commonwealth University, Richmond, VA, United States*
[d] *Department of Human and Molecular Genetics, Virginia Commonwealth University, Richmond, VA, United States*

*Student: williamska5@vcu.edu**
Mentor: thomasns@vcu.edu

ABSTRACT
Alcohol consumption is common in college attending populations and can have a negative impact on an individual's academic, physical, and mental health. Previous research suggests that living at home could act as a protective measure. The current research looks at potential mediators of the association between living with parents while attending college and amount of alcohol consumed. In particular, this study examined access to alcohol, parental involvement, and perception of peer drinking as mediators of the association. This study examined freshman data collected from a survey conducted at a large public university in the mid-Atlantic United States. A pathway model was fit to test the relationships between residence status, access to alcohol, parental involvement, and perception of peer drinking on alcohol consumption. We observed statistically significant indirect effects of residence status on alcohol consumption through the perception of peer drinking and access to alcohol. Parental involvement was significantly related to lower alcohol consumption and there was a direct effect of residence status on alcohol consumption. There were significant indirect effects of residence status on alcohol consumption through both peer drinking and access to alcohol. Parental involvement was associated with decreased alcohol consumption, with no indirect effect in association with residence status. These effects were persistent in the presence of a range of covariates, including age, gender, ethnicity, and parental education.

KEYWORDS: Emerging Adult; Alcohol; Residence Status; Peer Drinking; Access to Alcohol; Parental involvement; Path Analysis

INTRODUCTION

According to the Centers for Disease Control (CDC), the use of alcohol and illegal substances represent a considerable burden to public health.[1] Data published through the CDC indicate that in 2006 excessive drinking equated to an average of $746 of public health spending per person per year and is associated with upwards of 50 or more distinct injuries and diseases, such as car accidents, sexually transmitted diseases, and alcohol dependence.[1] Prevalence estimates from the past decade suggest that roughly 40% of college students endorse episodic heavy drinking in the past month.[2, 3] Relatedly, 18% of college students report experiencing clinically-significant problems with alcohol use.[4]

The consequences associated with heavy alcohol use in college-attending, emerging adult populations are stark. Excessive alcohol use is associated with lower GPA, [5, 6] discontinuous enrolments in third- and fourth-year students,[7] and select neurocognitive deficits.[8] Emerging adulthood also often represents a critical period in psychosocial and behavioral development, where relatively persistent trajectories in behavior and pathology are likely to begin.[9] Thus, excessive alcohol use in emerging adult college students may represent both an acute threat to academic performance, as well as a risk factor for problems with alcohol later in development.

Multiple reasons have been posited for why college attendance is associated with increased alcohol use. The increase in alcohol consumption in college-attending populations is often attributed to an increase in independence and relative lack of adult responsibilities such as full-time employment and child-rearing; although the Transition Catalyst Model suggests that this increase in alcohol consumption is due to a desire to acclimate to the new situations and circumstances that colleges students find themselves in.[10, 11] As college students enter into an environment associated with higher alcohol consumption, they may drink more in the process of acclimation. Despite the fact that many college students consume more alcohol during their time in college, there is a small portion of individuals that do not follow this particular trend. Individuals who live at home during their

college-attending years have a lower prevalence of risky patterns alcohol use, such as binge drinking and blacking out. These individuals also report overall lower alcohol consumption than their college-attending peers who live on campus.[12]

When examining college-attending populations, many studies define living at home as a controlled environment, or a living circumstance that minimizes risk factors for hazardous behavior. Operationally, Wechsler, et al. (2002) defines a controlled living environment as a substance-free residence hall or off-campus with parents; statistics on this population are often not exclusive to those living at home, but rather all college students who live in a controlled environment. [13] It is feasible that this operationalization of a controlled living environment homogenizes important variation within this broader group, failing to measure contextual nuance unique to living with one's parents. In the current analyses, we focus specifically on those individuals living with their parents.

Previous research suggests that living with parents could decrease a college student's risk of consuming excessive amounts of alcohol.[12] The increased parental influence was seen as a possible protective measure that reduced the amount of alcohol that a college student would drink.[14] Another study conducted by Baer, et al. (1991) found that those under the legal drinking age were less likely to drink if they knew that they would receive negative consequences from their parents (such as a lecture or punishment).[15] Most of the individuals involved in the study consumed less alcohol so that they would not receive the negative consequences from their parents, suggesting that this residence status may represent a protective factor from excessive alcohol use.

Additional research provides evidence of other factors that may contribute to this relationship, including perceptions of peer drinking, access to alcohol, and parental involvement. Many college students' perception of how much their peers drink is incorrect.[15] Many have a misconstrued perception of how much their peers drink, which then impacts how they view drinking more generally; individuals who believe that their peers consume excessive amounts of alcohol are more likely to adhere to these perceived social norms and consume excessive amounts of alcohol as well.[16] Living with one's parents may buffer college students from this misperception, as individuals may spend less time in social situations where alcohol consumption is considered normative, and establish social groups with individuals that their parents would approve of.[17] This often means that the individuals with fewer maladaptive social connections exhibit fewer risky alcohol use behaviors.[18] Generally, socializing with others that do not consume alcohol excessively encourages different perceptions of peer drinking, which may dispose these individuals to drink less.

Variation in the extent of college students' access to alcohol may further distinguish students living at home from students living on campus. For those who are under the legal drinking age—21 in the United States—obtaining alcohol requires access to some form of an illicit channel. By utilizing a variety of methods, such as using fake IDs or finding bars that do not check IDs, to obtain alcohol, half of college students under the legal drinking age report that alcohol is very easy to obtain, despite legal restrictions.[12] For a college student living at home, it may be harder to utilize these methods to obtain alcohol. They may be dissuaded from maintaining a fake ID for fear a parent could find it. They may not have access to stores or bars/clubs that do not card due to living off campus away from locations with a higher density of venues to purchase alcohol.[19] Furthermore, they may not know an of-age individual who is willing to purchase alcohol for them. All of these would reduce the accessibility of alcohol for this population, making it less likely that they would struggle with the same risky behaviors from which college students living on campus may engage in.

The protective effects of parental involvement are also well-supported in the literature. Low parental involvement is associated with both the initiation of alcohol use and transition to heavy drinking in adolescence.[20,21] Arria et al. (2008) report that level of high school drinking mediates the relationship between parental involvement in adolescence and college drinking, while other findings indicate the parental involvement in high school exerts a direct influence on college drinking.[22,23] These findings suggest that early parental involvement may continue to influence behavior into college by setting a precedent for one's drinking early on. Notably, few studies have examined the relationship between continuing to living with one's parents into college and high school parental involvement.

Previous research has shown that college students who live with their parents have a lower rate of alcohol consumption. It has also been seen that parental involvement has a significant role in the decreased alcohol consumption seen in that population. This study will test multiple mediators through a pathway model to determine if perceptions of peer drinking and access to alcohol have an effect on how much alcohol a college student living at home consumes. We hypothesize that 1) perceptions of peer drinking and 2) report of student's ease of access to alcohol will mediate the relationship between living with one's parents and grams of ethanol consumed per month, after accounting for the effect of parental involvement.

METHODS AND PROCEDURES

Data Source

The current analyses use data from The Spit for Science project, a longitudinal survey of undergraduate college students from a single university which assesses various aspects of behavioral and emotional health.[24] The project was launched in 2011 and, at this point, includes four cohorts of undergraduate students. Initial self-report data were collected in the fall semester of incoming freshmen's first year, with follow up assessments at every subsequent spring semester. This procedure was applied to each incoming cohort. Self-report data were collected using an electronic survey programmed in the Research Electronic Data Capture (REDcap) software. Participants are offered $10 to complete the electronic survey. The Spit for Science sample is generally representative of the demographic characteristics of the university's undergraduate population in terms of sex and race/ethnicity.[24] Further details, including full explication of the theoretical underpinnings of the broader project, recruitment activities utilized to increase enrollment, and a discussion of selected measures can be found in Dick et al. (2014).[24] This study was approved by the university's Institutional Review Board. Participants were presented with consent documentation and indicated that they understood the potential risks and benefits of participating.

Measures

Covariates

Demographic information included age, gender, race/ethnicity, and highest education achieved by each of subjects' parents.

Residence

Subjects' residence was assessed with a single item in the Fall semester of subjects' first year in college which read "Where do you live while attending university?", with response options "*Residence Hall*", "*Off-campus housing*", "*Parent's house*", and "*Other*". This measure was then used to calculate an indicator for endorsement of the "*Parent's house*" category, to be compared with subjects endorsing any of the other categories.

Steinberg Parenting Style, Parental Involvement

Parental involvement was assessed in the Fall semester of subjects' first year in college using the Involvement subscale of the Steinberg Parental Style inventory.[25] This subscale is comprised of three items. The first item read, "My parents helped me with schoolwork if there was something I didn't understand." The second item read, "My parents knew who my friends were". The third item read, "My parents spent time just talking with me". Response options for these three items were (1) "*Strongly Agree*", (2) "*Agree somewhat*", (3) "*Disagree somewhat*", (4) "*Strongly Disagree*". Scores on these items were summed after being reverse coded, such that a higher sum score would reflect greater parental involvement (α=0.68). Missing data were pro-rated if a given subject had answered at least two of the three items. The resulting sum score had a minimum value of three and a maximum value of 12.

Peer Drinking

Peer drinking was assessed in the Spring semester of subjects' first year in college with a single item which read "The following question are about your friends – friends you would have seen regularly and spent time with in school or outside of school. Please answer for your friends that you spend time with since starting school. How many of your friends have done the following? How many would have drunk alcohol?" with response options (1) "*None*", (2) "*A few*", (3) "*Some*", (4) "*Most*" and (5) "*All*".

Access to Alcohol

Access to alcohol was assessed with a single item in the Spring semester of subjects' first year in college which read, "How easy is it for you to obtain alcohol currently?", with response options (1) "*Very difficult*", (2) "*Difficult*", (3) "*Easy*" and (4) "*Very easy*".

Grams of ethanol consumed per month

Grams of ethanol consumed per month was calculated from separate measures of quantity and frequency of alcohol consumption in the Spring semester of subjects' first year in college. Frequency of alcohol consumption was measured with one categorical item, "How often do you have a drink containing alcohol?", with response options "*Never*", "*Monthly or less*", "*2 to 4 times a month*", "*2 to 3 times a week*", and "*4 or more times a week*". Quantity of alcohol consumption was measured with one categorical item, "How many drinks containing alcohol do you have on a typical day when you are drinking?", with response options "*1 or 2*", "*3 or 4*", "*5 or 6*", "*7, 8, or 9*", and "*10 or more*".

Together, these ranges were converted to a measure of grams of ethanol consumed per month using a procedure described in previous literature.[26,27] Frequency categories were converted to the median of the range of each response option to reflect drinking occasions per month, i.e. "*Never*" = 0, "*Monthly or less*" = 0.5, "*2-4 times a month*" = 3, "*2-3 times a week*" = 10.7. The "*4 or more times a week*" category was set equal to 23.54, based on the average count of 4.28 weeks per month, for a possible range of 17.12- 29.96 drinking days per month Drinking quantity was quantified using a similar procedure, i.e. "*1 or 2*" =1.5, "*3 or 4*" = 3.5, "*5 or 6*" = 5.5, "*7, 8, or 9*" = 8. The "*10 or more*" category was set equal to 15 based on the specification of 21 as the upper limit of drinks per occasion, in alignment with a similar continuous measure in the Spit for Science survey.

The product of recoded frequency and quantity was then multiplied by 14, which represents the grams of ethanol contained in a single, standard drink in the United States. These calculations were applied to each individual's data on quantity and frequency. The resulting measure is a pseudo-continuous measure of alcohol consumption that may adopt 25 different values. Grams of ethanol consumed per month was transformed by the natural log, plus a constant of 1 to retain individuals who reported no past month alcohol use to limit distributional problems associated with outliers in this measure.

Data Analysis

A path analysis was conducted to test mediational hypotheses in R using the "lavaan" package. Estimation by maximum likelihood allowed the use of the full sample (n=9,889). All regressions in the model controlled for mother's education, father's education, age, gender, and ethnicity.

Indirect effects were calculated in "lavaan" as the product of corresponding path coefficients. All reported coefficients were standardized to facilitate clear interpretation.

RESULTS

Sample Composition

The sample used in the current analyses was drawn from 4 cohorts of longitudinal data collected between the years 2011-2014 at a public university in the Mid-Atlantic region of the United States (total n=9,889). Maximum likelihood estimation permits the use of subjects with incomplete data and sample size varies to some extent between measures; a complete description of the sample can be found in **Table 1**. All measurements were drawn in the Fall or Spring of students' first year of college.

Path model

Multiple fit indices suggest that the specified model fit our data exceptionally well (Chi-square P-value=0.246; RMSEA= 0.006, 90% CI: (0, 0.022); CFI= 1.00).

Effect sizes were standardized for interpretability. Broadly, the hypotheses laid out in the current manuscript were supported. We observed a statistically significant indirect effect of residence status on alcohol consumption through the perception of peer drinking (beta=-0.494, P=<0.001), to suggest that living with one's parents reduces perceptions of perceived peer drinking on alcohol use. Similarly, we observed a statistically significant indirect effect of residence status on alcohol consumption through access to alcohol (beta=-0.102, P<0.01), to suggest that living with one's parents may limit access to alcohol and—subsequently—reduce alcohol use. No indirect effect through parental involvement was observed, although parental involvement itself was significantly related to lower alcohol consumption (beta= -0.031, P<0.01). These relationships did not fully explain the relationship between residence status and alcohol consumption; we also observed a direct effect of residence status on alcohol consumption (beta= -0.617, P=<0.001). Complete explication of model coefficients can be found in **Figure 1**.

Sensitivity Analyses

An additional iteration of the path model with covariates removed was run to assess the effect of included demographic covariates on results. Results from this model suggest that the patterns of association we have observed are generally robust. The path model without covariates replicated previously observed indirect effects of residence status on alcohol use through the perception of peer drinking (beta=-0.636, p<0.001) and access to alcohol (beta=-0.172, P=0.002). Again, there was no indirect effect associated with involved parenting style and the direct effect of involved parenting style to alcohol consumption did not reach statistical significance (beta=-.024, P=0.06). A direct effect of residence on alcohol use remained (beta=-0.609, P<0.001).

Measure		Total Sample	Living with parents	Living elsewhere
Gender*				
	Total n	9820	7832	
	Male	3780 (38.5%)	184 (2.3%)	2768 (35.3%)
	Female	6040 (61.5%)	285 (3.6%)	4595 (58.7%)
Ethnicity*				
	Total n	9750	7741	
	White	4881 (50.1%)	255 (3.3%)	3745 (48.4%)
	Asian	1615 (16.6%)	111 (1.4%)	1145 (14.8%)
	Black/African American	1873 (19.2%)	55 (0.7%)	1395 (18.0%)
	Hispanic/Latino	594 (6.1%)	22 (0.2%)	455 (5.9%)
	Other Ethnicity	787 (8.1%)	24 (0.3%)	534 (6.9%)
Residence				
	Total n	7865		
	With parents	471 (6.0%)		
	Elsewhere	7394 (94.0%)		

Table 1. Frequencies for measures used in the analysis. Covariates marked with an asterisk

Measure		n	Mean	SD
Involved Parenting Style				
	Total	7399	9.61	2.08
	Living with Parents	366	9.5	2.14
	Living Elsewhere	5559	9.59	2.09
Peer Drinking				
	Total	7423	3.19	1.22
	Living with Parents	319	2.56	1.21
	Living Elsewhere	5165	3.19	1.19
Access to Alcohol				
	Total	4121	3.12	0.76
	Living with Parents	194	2.96	0.84
	Living Elsewhere	3890	3.13	0.76
Grams of ethanol consumed per month				
	Total	6016	265.3 (19)	525.3 (38)
	Living with Parents	319	101.7 (7)	275.62 (20)
	Living Elsewhere	4242	260.6 (19)	510.92 (36)

Table 2. Descriptive statistics. Descriptive statistics for grams of ethanol (approx. drinks)

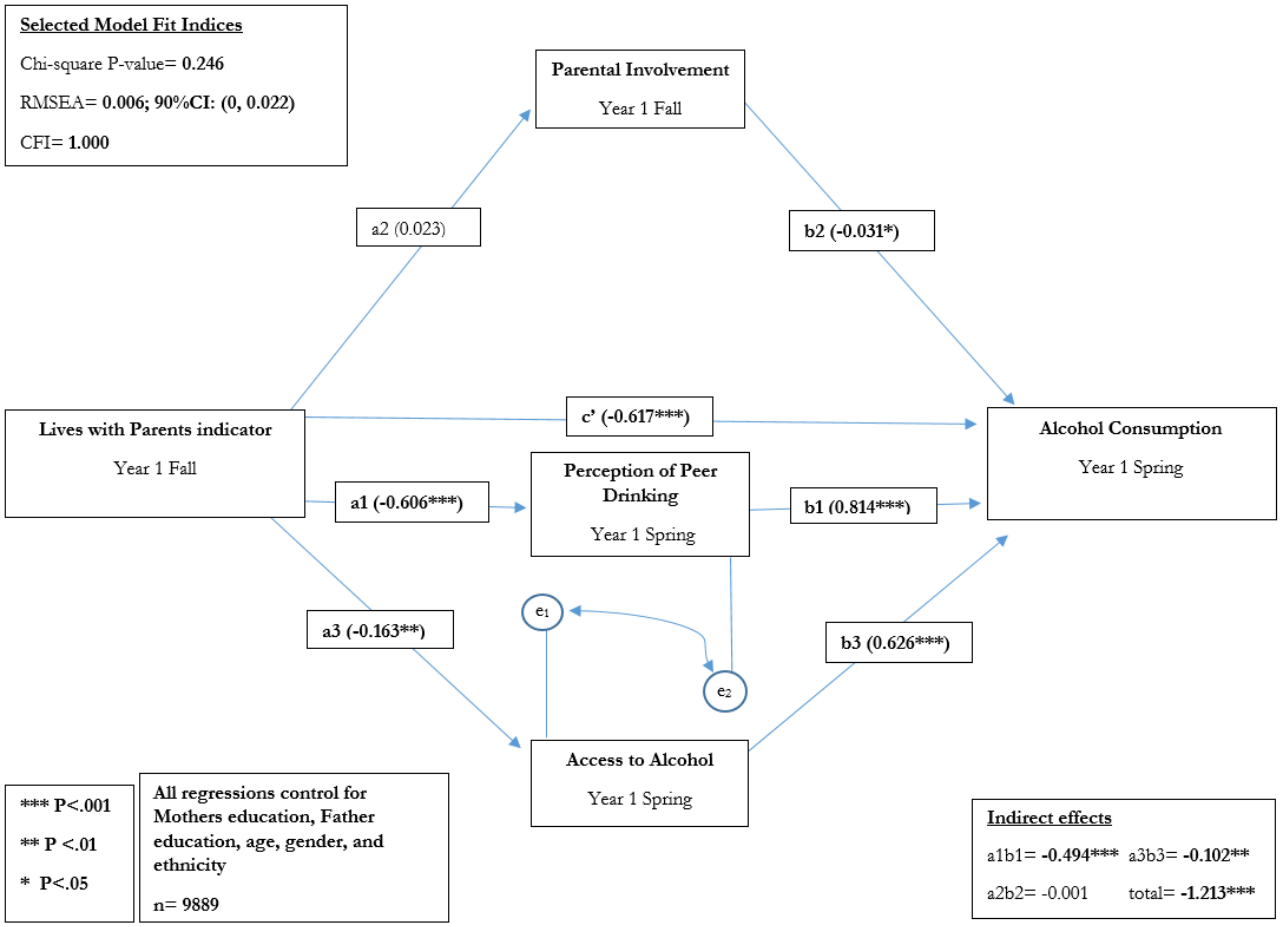

Figure 1. Path model. Perception of Peer Drinking mediates the relationship between living with one's parents and Alcohol Consumption (a1b1 path). Similarly, Access to Alcohol mediates the relationship between living with one's parents and Alcohol Consumption (a3b3 path). Parental involvement does not mediate the relationship between living with one's parents and Alcohol Consumption (a2b2 path). After accounting for these relationships, a direct effect of living with one's parents on Alcohol Consumption remains (c' path).

DISCUSSION

Key Findings

In general, the hypotheses laid out in the current manuscript were well supported in our analyses. We hypothesized that 1) perceptions of peer drinking and 2) report of student's ease of access to alcohol would mediate the relationship between living with one's parents and grams of ethanol consumed per month. We observed significant indirect effects of residence status, through both peer drinking and access to alcohol, on alcohol consumption. Parental involvement was associated with decreased alcohol consumption. These effects were persistent in the presence of a range of covariates, including age, gender, ethnicity, and parental education.

The protective effects of living with parents were partially explained by these two mediators. Living with one's parents had an indirect effect on alcohol consumption through the perception of peer drinking and access to alcohol. Living with one's parents was associated with lower perceptions of peer drinking, suggesting that parents play an important role in deciding with whom an individual spends time. Through this mediated association, living with one's parents affects perceived peer drinking. In the same way, living with one's parents affects access to alcohol, which is also associated with lower consumption of alcohol.

Practical Applications

In some capacity, the benefits of living with one's parents—reduced alcohol use because of lower perceptions of peer alcohol use and less access to alcohol—may be extended to students living on campus by influencing their social environments. Social norms campaigns that reduce the perception of peer alcohol use may subsequently reduce alcohol use in students. It is possible that social norms campaigns can reduce alcohol consumption in the college attending population by changing the way that college

students, freshmen in particular, view alcohol and their peer's consumption of alcohol. Current research suggests that social norm campaigns may not be as effective as once thought, although other findings suggest that social norm campaigns are more effective on campuses with a lower density of alcohol sales venues around campus. [28,29] In cases where alcohol sales venue density is higher, or unknown, it may be more effective to use other programs focused on preventing risky alcohol behavior, such as the Brief Alcohol Screening Intervention for College Students (BASICS).[30] Another way that universities can reduce alcohol consumption through policy change is by implementing more substance-free housing- and strictly enforcing the standards in these residence halls. While some universities already have these options, the substance-free policies are not always consistently enforced, leading to greater access to alcohol. Our results suggested that limited access to alcohol is one benefit of livings with one's parents while attending college; it may stand to reason that university residence halls can emulate this protective effect by placing stricter controls on students' alcohol use.

Limitations

We observed partial mediation in the current analyses, rather than fully accounting for the effect of residence status on alcohol consumption through indirect effects. There are two possible explanations for the partial mediation. It is possible that residence status in-and-of-itself has a direct effect on alcohol consumption. Otherwise, it is possible that there are additional mediating variables that facilitate the apparent effect of residence status on alcohol consumption. It may be more likely that the second possibility is the cause of the partial mediation, as there are many factors that contribute to alcohol consumption. Future analyses should aim to test other candidate measures to determine what other factors mediate alcohol consumption in college-attending populations.

The proportion of the study population endorsing the "Lives with parents" category represents a further limitation. Individuals who live off campus are less likely to complete surveys than those living on campus (62% of on-campus, first students were enrolled, compared to 36% of students living off-campus).[24] Based on that, our sample size was adequate, but our cell size for those living with parents was smaller. The smaller cell size could have had an impact on our results, and the results we observed might not represent the student body overall. Samples with a larger proportion of students living with their parents may be necessary to generalize these findings to the broader population of students living with their parents.

The outcome measure of these analyses, grams of ethanol consumed per month, was calculated from 2 ordinal measures of quantity and frequency. Subsequently, the combination of these measures lacks some degree of precision. As with any self-report survey data, subjective bias may also influence responses. The information gathered in this study did not take into consideration individuals who identified as non-binary in regards to gender. This did limit the results of the study to those who identified as male or female. To address this in future studies, questionnaires should provide more identifying options to students. Lastly, measurements were drawn from a single year of data collection; subsequently, the results of these analyses should be interpreted as correlational in nature.

Future Directions

The relationship between residence status and alcohol consumption is partially accounted for by indirect effects through access to alcohol and perceptions of peer drinking. A remaining direct effect between living with parents and alcohol consumption suggests the existence of other mediating variables not accounted for in these analyses. Future analyses might use a broader range of measures to explain a larger proportion of the relationship in question. Additionally, identifying college samples from universities with a higher proportion of individuals who live at home, or utilization of sampling strategies aimed at recruiting more of these potential subjects may be beneficial in future projects. With a large sample of college students living at home, future investigations may explore heterogeneity within this population; differences in subjects' motivations for living at home may be important determinants of alcohol use in college.

ACKNOWLEDGEMENTS

The authors thank Dr. Jessica Salvatore for critical suggestions and edits to the text of this manuscript, as well as Dr. Danielle Dick and Dr. Kenneth Kendler for supporting the Spit for Science project.

Spit for Science: The VCU Student Survey has been supported by Virginia Commonwealth University, P20 AA017828, R37AA011408, K02AA018755, and P50 AA022537 from the National Institute on Alcohol Abuse and Alcoholism, and UL1RR031990 from the National Center for Research Resources and National Institutes of Health Roadmap for Medical Research. We would like to thank the VCU students for making this study a success, as well as the many VCU faculty, students, and staff who contributed to the design and implementation of the project.

REFERENCES

1. Centers for Disease Control and Prevention, Binge Drinking: Nationwide Problems, Local Solutions, (2013), *https://www.cdc.gov/vitalsigns/BingeDrinking/index.html* (accessed Nov 2016)
2. O'Malley, P. M., Johnston, L. D. (2002) Epidemiology of Alcohol and Other Drug Use among American College Students. *J Stud Alcohol* 14, 23–39. DOI: *http://dx.doi.org/10.15288/jsas.2002.s14.23*
3. White, A., Hingson, R. (2014) The Burden of Alcohol Use: Excessive Alcohol Consumption and Related Consequences Among College Students. *Alcohol Res* 35(2), 201–218.
4. Slutske, W. S. (2005) Alcohol Use Disorders Among US College Students and Their Non-College-Attending Peers. *Arch Gen Psychiatry* 62(3), 321–327. DOI: *https://doi.org/10.1016/s0084-3717(08)70186-7*
5. Musgrave-Marquart, D., Bromley, S. P., Dalley, M. B. (1997) Personality, academic attribution, and substance use as predictors of academic achievement in college students. *J Soc Behav Pers* 12(2), 501–511.
6. Williams, J., Powell, L. M., Wechsler, H. (2003) Does alcohol consumption reduce human capital accumulation? Evidence from the College Alcohol Study. *Appl. Econ.* 35(10), 1227–1239. DOI: *https://doi.org/10.1080/0003684032000090735*
7. Arria, A. M., Caldeira, K. M., Vincent, K. B., Winick, E. R., Baron, R. A., O'Grady, K. E. (2013) Discontinuous college enrolment: associations with substance use and mental health. *Psych Serv* 64(2) 165–172. DOI: *https://doi.org/10.1176/appi.ps.201200106*
8. Zeigler, D. W., Wang, C. C., Yoast, R. A., Dickinson, B. D., McCaffree, M. A., Robinowitz, C. B., Sterling, M. L. (2005) The neurocognitive effects of alcohol on adolescents and college students. *Prev. Med. 40*(1), 23–32. DOI: *https://doi.org/10.1016/j.ypmed.2004.04.044*
9. Schulenberg, J. E., Sameroff, A. J., Cicchetti, D. (2002) The transition to adulthood as a critical juncture in the course of psychopathology. *Dev. Psychopathol* 1(4), 799–806. DOI: *https://doi.org/10.1017/s0954579404040015*
10. Sussman, S., Arnett, J.J. (2014) Emerging adulthood: developmental period facilitative of addictions. *Eval. Health Prof* 37(2), 147–155. DOI: https://doi.org/10.1177/2167696815587422
11. Schulenberg, J.E., Maggs, J.L. (2002) A developmental perspective on alcohol use and heavy drinking during adolescence and the transition to young adulthood. *Journal of Studies on Alcohol and Drugs* (14), 54-70. DOI: https://doi.org/10.15288/jsas.2002.s14.54
12. Cooke, M.E., Neale, Z.E., Barr, P.B., Myers, J., Dick, D.M., Kendler, K.S., Edwards, A.C. (2016). The role of social, familial, and individual-level factors on stages of alcohol use during the first year of university (Unpublished) Virginia Commonwealth University, Richmond, VA.
13. Wechsler, H., Lee, J.E., Nelson, T.F., & Kuo, M. (2002) Underage College Students' Drinking Behavior, Access to Alcohol, and the Influence of Deterrence Policies. *J Am Coll Health* 50(5), 223. DOI: *https://doi.org/10.1080/07448480209595714*
14. Merrill, J.E., Cary, K.B. (2016) Drinking over the lifespan: focus on college ages. *Alcohol Res,* 38(1), 103–114.
15. Baer, John S., Stacy, A., Larimer, M. (1991) Biases in the perception of drinking norms among college students. *J Stud Alcohol* 52(6), 580–586. DOI: https://doi.org/10.15288/jsa.1991.52.580
16. Ross, L., Green, D. and House, P. (1977) The "False Consensus Effect": An Egocentric Bias in Social Perception and Attribution Processes. *J. Exp. Soc. Psychol* 13, 279–301. DOI: *https://doi.org/10.1016/0022-1031(77)90049-x*
17. Mounts, N. S. (2002). Parental management of adolescent peer relationships in context: The role of parenting style. *Journal of Family Psychology, 16*(1), 58-69. http://dx.doi.org/10.1037/0893-3200.16.1.58
18. Rulison, K.L., Wahesh, E., Wyrick, D.L., DeJong, W. (2016) Parental influence on drinking behaviors and the transition to college: the mediating role of perceived friend's approval of high risk drinking. *J. Stud. Alcohol Drugs* 77(4), 638–648. DOI: *https://doi.org/10.15288/jsad.2016.77.638*
19. Harford, T.C., Wechsler, H., Seibring, M. (2002) Attendance and alcohol use at parties and bars in college: a national survey of current drinkers. *J Stud Alcohol* 63(6), 726–733. DOI: *https://doi.org/10.15288/jsa.2002.63.726*
20. Steinberg, L., Fletcher, A., Darling, N. (1994) Parental involvement and Peer Influences on Adolescent Substance Use. *Pediatr.* 93(6), 1060–1064. DOI: *https://doi.org/10.1017/cbo9780511527906.016*
21. Reifman, A., Barnes, G. M., Dintcheff, B. A., Farrell, M. P., Uhteg, L. (1997) Parental and Peer Influences on the Onset of Heavier Drinking among Adolescents. *J Stud Alcohol* 59(3), 311–317. DOI: *https://doi.org/10.15288/jsa.1998.59.311*
22. Arria, A. M., Kuhn, V., Caldeira, K. M., O'Grady, K. E., Vincent, K. B., Wish, E. D. (2008) High school drinking mediates the relationship between parental involvement and college drinking: A longitudinal analysis. *Subst Abuse Treat Prev Policy,* 3(6). DOI: *https://doi.org/10.1186/1747-597x-3-6*
23. Kaynak, O., Meyers, K., Caldeira, K. M., Vincent, K. B., Winters, K. C., Arria, A. M. (2013) Relationships among parental involvement and sensation seeking on the development of substance use disorders among college students. *Addict Behav* 38(1), 1457–1463. DOI: *https://doi.org/10.1016/j.addbeh.2012.08.003*
24. Dick, D. M., Nasim, A., Edwards, A. C., Salvatore, J. E., Cho, S. B., Adkins, A…Kendler, K. S. (2014) Spit for Science: launching a longitudinal study of genetic and environmental influences on substance use and emotional health at a large US university. *Front Genet.* 5(47), 1–12. DOI: *https://doi.org/10.3389/fgene.2014.00047*

25. Steinberg, L., Lamborn, S.D., Dornbusch, S.M. & Darling, N. (1992). Impact of Parenting Practices on Adolescent Achievement: Authoritative Parenting, School Involvement, and Encouragement to Succeed. *Child Dev.* 63, 1266–1281. DOI: *https://doi.org/10.2307/1131532*

26. Salvatore, J. E., Thomas, N. S., Cho, S. B., Adkins, A., Kendler, K. S., & Dick, D. M. (2016) The role of romantic relationship status in pathways of risk for emerging adult alcohol use. *Psychol Addict Behav* 30(3), 335–344. DOI: https://doi.org/10.1037/adb0000145

27. Dawson, D.A. (2011) U.S. low-risk drinking guidelines: An examination of four alternatives. *Alcoholism: Clinical and Experimental Research*. 2000a;24:1820–1829. DOI: 10.1111/j.1530-0277.2000.tb01986.x

28. Wechsler, H., Nelson, T. F. (2008) What We Have Learned From the Harvard School of Public Health College Alcohol Study: Focusing Attention on College Student Alcohol Consumption and the Environmental Conditions That Promote It. *J. Stud. Alcohol Drugs* 69, 481–490. DOI: *https://doi.org/10.15288/jsad.2008.69.481*

29. Scribner, R. A., Theall, K. P., Mason, K., Simonsen, N., Schneider, S. K., Towvim, L. G.... DeJong, W. (2011) Alcohol Prevention on College Campuses: The Moderating Effect of the Alcohol Environment on the Effectiveness of Social Norms Marketing Campaigns. *Journal of Studies on Alcohol and Drugs,* 72(2), 232–239. DOI: *https://doi.org/10.15288/jsad.2011.72.232*

30. Fachin, A., Aliane, P.P, Martinez, E.Z., Furtado, E.F. (2012) Efficacy of brief alcohol screening intervention for college students (BASICS): a meta-analysis of randomized controlled trials. *Substance Abuse Treatment, Prevention, and Policy*, 7:40 https://doi.org/10.1186/1747-597X-7-40

31. Hermida, R. (2015) The problem of allowing correlated errors in structural equation modeling: concerns and considerations. *CMSS* 3(1), 5–17.

ABOUT THE STUDENT AUTHOR

Katrina Williams worked on this project as an intern with the Spit for Science lab at Virginia Commonwealth University during her senior year. She graduated from Virginia Commonwealth University in December of 2016, with a Bachelor of Science degree in Health and Physical Education with a concentration in Exercise Science. She is currently enrolled in Virginia Commonwealth University's Entry-level Occupational Therapy Doctorate (EL-OTD) program, with a goal of working with the pediatric special needs community.

PRESS SUMMARY

It is easy to assume that the association between residence status and alcohol use is due to the fact that the college student is living with their parents, and the parents, therefore, are having a large impact on how much their child drinks. Recent studies have shown that this may not be the case. This study looked at other reasons why a college student who lives at home may drink less alcohol than those who do not live at home during their college attending years. This study focused on two factors: how much alcohol college students think other college students drink and how easy alcohol was to obtain. Data were drawn from freshmen attending a four-year university in an urban mid-Atlantic region. The data obtained from these surveys was then used to determine how these factors influence the amount of alcohol that college students who live with their parents consume. Lower perceptions of peer drinking and less access to alcohol in students living with their parents were shown to reduce overall alcohol consumption, relative to students living on campus. While other factors may also play a role in explaining reduced alcohol use in students living with their parents, perceptions of peer drinking and access to alcohol appear to be strong contenders to begin to unwind this apparent trend.

Speedup Potential for Reconstruction Techniques for Prompt Gamma Imaging During Proton Radiotherapy

James Della-Giustina[*a], *Johnlemuel Casilag*[b], *Elizabeth Gregorio*[c], *Aniebiet Jacobs*[b]

[a]*Department of Information Technology & Computer Science, Community College of Baltimore County, Baltimore, MD*
[b]*Department of Computer Science & Electrical Engineering, University of Maryland, Baltimore County, Baltimore, MD*
[c]*Department of Physics, Hamline University, St. Paul, MN*
[d]*Department of Mathematics and Statistics, University of Maryland, Baltimore County, Baltimore, MD*
[e]*Department of Radiation Oncology, University of Maryland School of Medicine, Baltimore, MD*
[f] *Department of Radiation Physics, The University of Texas MD Anderson Cancer Center, Houston, Texas*

Students: jdella@umbc.edu, cas6@umbc.edu, anie1@umbc.edu, egregorio01@gmail.com*
Research Assistant: Carlos Barajas[d], *barajasc@umbc.edu*
Faculty Mentor: Matthias K. Gobbert[d], *gobbert@umbc.edu*
Clients: Dennis Mackin[f] , *dsmackin@mdanderson.org, Jerimy Polf*[e], *jpolf@umm.edu*

ABSTRACT
Proton beam radiation treatment was first proposed by Robert Wilson in 1946. The advantage of proton beam radiation is that the lethal dose of radiation is delivered by a sharp increase toward the end of the beam range. This sharp increase, known as the Bragg peak, allows for the possibility of reducing the exposure of healthy tissue to radiation when comparing to x-ray radiation treatment. As the proton beam interacts with the molecules in the body, gamma rays are emitted. The origin of the gamma rays gives the location of the proton beam in the body, therefore, gamma ray imaging allows physicians to better take advantage of the benefits of proton beam radiation. These gamma rays are detected using a Compton Camera (CC) while the SOE algorithm is used to reconstruct images of these gamma rays as they are emitted from the patient. This imaging occurs while the radiation dose is delivered, which would allow the physician to make adjustments in real time in the treatment room, provided the image reconstruction is computed fast enough. This project focuses on speeding up the image reconstruction software with the use of of parallel computing techniques involving MPI. Additionally, we demonstrate the use of the VTune performance analyzer to identify bottlenecks in a parallel code.

KEYWORDS
Proton Beam Therapy; Image Reconstruction; SOE Algorithm; Parallel Computing; High Performance Computing; Medical Imaging; Prompt Gamma Imaging; Radiotherapy

1. INTRODUCTION

In order for physicians to ensure accurate treatment, it is essential for them to have images of the patients anatomy taken throughout the administration of radiation therapy. This is necessary because, as a patient undergoes treatment, their anatomy changes as the tumor shrinks and surrounding tissue swells. This means that each day during treatment the target for the radiation may be slightly different. Therefore, if a physician were to have the ability to see where inside of the body the proton beam is delivering its dose while in the treatment room they would be able to more accurately treat patients. It is possible for physicians to attain this information through prompt gamma imaging of the proton beam and image reconstruction.

Prompt gamma imaging works by capturing the scattered gamma rays released when a proton beam interacts patients cells and applying the Stochastic Origin Ensemble (SOE) algorithm. These gamma rays are released while the proton beam is being administered to the patient, therefore, this imaging must be done at the same time as treatment. Because the gamma

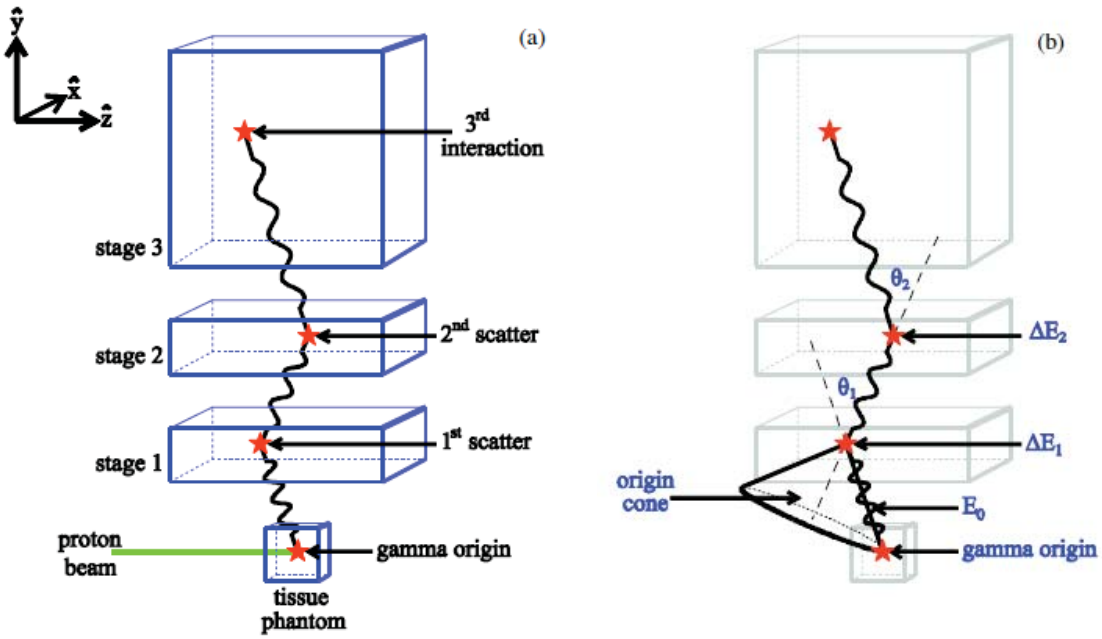

First stage reconstruction Second stage reconstruction

Figure 1. Gamma ray scatter and its image reconstruction.

rays are released where the proton beam interacts with the patient, the origins of these gamma rays are in the same position within the body as the proton beam. Therefore, if the origins of the rays can be traced back and compiled to construct an image, then physicians will have the ability to see exactly where the proton beam is delivering its dose of radiation. In a clinical setting, this imaging offers doctors the possibility of making adjustments to the treatment of patients in real time.[1] Being able to make these adjustments will allow them to better take advantage of the potential for a proton beam to deliver smaller doses of radiation to surrounding healthy tissue.

In order for the proton beam to hit the specified volume of tissue it is necessary for the patient to lie entirely still on the treatment table. It is also necessary for them to lie still during imaging as imaging occurs while the proton beam is being administered. The position a patient needs to hold can often be difficult or awkward be in for long periods of time. Therefore, it is important that this imaging software runs as fast as possible.[2, 3] This project explores the possibility for implementation of parallelism to the image reconstruction software through the development of an MPI algorithm to decrease this run time.

The remainder of this report is organized as follows: **Section 2** describes the SOE algorithm used for the image reconstruction and different versions of its implementation. **Section 3** presents results of the reconstructions using the different versions of the code and their performance results. **Section 4** summarizes our conclusions.

2. ALGORITHM AND IMPLEMENTATION

2.1. *SOE algorithm*

During data collection, gamma rays scatter into a specially designed camera known as a "Compton Camera" (CC) which records the coordinates and energy deposited by each gamma ray that interacts with the CC. Each gamma ray must interact with the camera at least two times to be useful for imaging. The 3D coordinates and energies deposited by the gamma rays are stored in a data file which is used to initialize the conic image reconstruction software. A line is drawn between the two points of ray impact and an angle is calculated and used to construct an initial cone as seen in **Figure 1**. The cone's surface encompasses all the possible origins for that ray. After these cones have been constructed, a random point from the surface of the cone is chosen as an initial guess for the likely origin of the gamma ray. This initial point becomes the algorithm's first guess for the likely origin of that gamma ray. The 3D area containing the tissue phantom seen in **Figure 1** is turned

into a 3D density histogram divided into bins. Lastly the density histogram is populated by the counts of all likely origins contained in each 3D bin.

The conic reconstruction, based on the SOE algorithm,[4] then improves the histogram iteratively by moving likely origins for each cone to more likely locations using the criterion of an already higher density in the histogram. That is, in each iteration, for each cone, the algorithm chooses a new random point in its cone of possible origins for that ray. If the random point has a higher density than the density of the current likely origin of that cone, it chooses the random point as the new likely origin of the cone. Correspondingly, the histogram is updated by decrementing the count in the old likely origin's bin and incrementing the count in the new likely origin's bin. These iterations are run until only a small fraction of likely origins is changed in one iteration.

2.2. *Description of code implementation*

Two input files are required to run this code. A configuration file controls various parameters for the code. Important parameters include the total number of cones used, histogram coordinate boundaries in the x, y, and z directions, the total number of bins in the x, y, z directions, and the total number of iterations; notice that the number of iterations is fixed here by trial and error based on observing a small enough fraction of likely origin changes. The configuration file also specifies the name of the second input file, which is obtained from the gamma ray scattering into the CC. This is the measured data file containing a list of the energy deposited and x, y, and z coordinates of each gamma ray interaction occurring in the CC during the measurement.

The initial cones are created using the process described in **Section 2.1** and their first likely origins are stored in an initial 3D density histogram. It then begins the iterations in which for each cone the algorithm picks a random coordinate point and checks if the histogram bin has a greater density than the cone's current bin. If so, the cones current bin is decremented, the new found bin is incremented, and the cone's likely origin is updated to be that of the new coordinate. The code writes the iteration number, the time elapsed, the numbers of cone origins updated, and the fraction of cones updated to the stdout. After the iterations have ceased, the code outputs the changes made into a file called `events.dat`. Additionally a file called `output.dat` is generated that provides coordinates of the last likely origin for each ray. Also the configuration file is saved for the run. All three output files are used for post-processing using Python2.7 that plots numerous figures. For comparison in **Section 3**, we use plots of likely origins of all cones.

2.3. *OpenMP algorithm*

The original code for this project was developed by Drs. Dennis Mackin and Jerimy Polf. The number of cones used is typically large, so that it makes sense to speed up their processing by distributing work to several computational cores of a node with two multi-core CPUs. This was accomplished in the original version of the code by using the shared-memory parallel library OpenMP. The program first obtains the initial cones and initial density histogram via **Section 2.1** in serial. At the start of the iterations, the OpenMP threads are started up using an OpenMP `parallel for` pragma applied to the loop over all cones. The cones are then distributed to each thread, which distributes the main work of the code for a potential speedup as large as the number of threads used. The number of threads used is limited to the number of computational cores of the two multi-core CPUs on one node, since OpenMP works only on a code that shares memory across all threads. This implies that the density histogram is shared between all threads at all times. Each thread will try to find a new origin, as in **Section 2.2**, for each cone, by comparing the density of the cone's current bin location to the new bin location. If the density of the new bin is greater, the code changes the likely origin of the cone and updates the histogram immediately by decrementing the old bin and incrementing the new bin. Since the histogram is in shared memory of all threads, OpenMP has to put a lock on the histogram, via a `critical` pragma, during this update, which forces other threads to idle during this time, thus decreasing parallel efficiency. But the latest histogram is always immediately available to all threads after the end of the lock, giving best convergence of the algorithm. After all cones have been processed, the threads shut down and the output to stdout is done as stated in **Section 2.2**. This is repeated until all iterations have been completed and the output files are generated as they were in **Section 2.2**.

2.4. *Original MPI algorithm*

The algorithm explained in **Section 2.3** was changed based on the observation that the density of a likely origin of a cone is defined as its bin number's count, thus we work directly with the histogram from now on. We replaced the use of OpenMP by MPI (Message Passing Interface), so that the parallel code is not limited by the number of cores of one node anymore, but can use several nodes with distributed memory. The parallelism is achieved just like with OpenMP by distributing the large number of cones to the MPI processes. Each MPI process holds the cone database including the likely origin of each cone for its own cones only, hence this does not increase the overall memory usage of the code. Since the histogram is not too large in memory, it is possible to give each process a local copy of the density histogram. Doing so cuts out extra communication amongst processes that would come with each process having sections of the histogram and it avoids the need for a lock as required by the shared memory structure of OpenMP.

In each iteration, the MPI process picks a random bin for its cone and checks its density using the local histogram against the old bin number in the local histogram. However each process does not change their local density histogram; the changes are instead tracked by a local count vector and the local histogram remains unchanged. This means that all density checks are happening against the local histogram from the previous iteration rather than the latest histogram used in the OpenMP version. The local count vectors are then combined into a global count vector using `MPI_Allreduce` every 1 iteration and all local histograms updated. At present, our MPI code does not combine the cone data from all processes back into a serial data structure used for the output files `events.dat` and `output.dat` used for Python post-processing. Instead, the histogram data itself is output every 100 iterations to file, and Matlab post-processing was created that plots the histogram data, i.e., the counts of the bins, instead of the coordinates of the likely origins.

2.5. *Modified MPI algorithm*

The only parallel cost of the MPI algorithm described in **Section 2.4** is the use of the `MPI_Allreduce` command after every iteration. We created a modified MPI algorithm that instead of updating the histograms after 1 iteration only updates it every 10 iterations. This has the potential for speeding up the execution time of the code significantly, i.e., in principle by a factor 10. The potential downside is that the convergence might be slower, that is, that more iterations might be needed to reach a histogram of the same quality as measured by the number of changes of likely origins needed in an iteration.

2.6. *Hardware utilized*

To measure performance of the software, we ran studies on the newest nodes of the Maya cluster in the UMBC High Performance Computing Facility (hpcf.umbc.edu). These nodes contain two Intel E5-2650v2 Ivy Bridge (2.6 GHz, 20 MB cache) CPUs and 64 GB of memory each and are connected by a low latency quad data rate (QDR) InfiniBand interconnect.

2.7. *Intel VTune*

To fully understand the time inefficiency of the code, we profiled the code using Intel's VTune software.[5] This performance profiler analyzes software in respect to many different areas of potential improvement. For our uses, we chose the HPC Performance Characterization analysis, as well as Hotspots analysis. These tests were run on the Texas Advanced Computing Center's (TACC) Stampede cluster, even though this report does not contain performance results from that cluster. These tests provide us data about how effectively our computationally intensive functions utilize memory, CPU, and hardware resources. This also provides information about the OpenMP and MPI parallelized performance efficiency within the code.

3. RESULTS

The following are the results were obtained from the different algorithms that are formulated in **Section 2**. Each algorithm uses the same deterministic configuration file utilizing 100,000 cones imaged by a histogram with $102 \times 102 \times 126$ bins.

3.1. *OpenMP algorithm*

The OpenMP algorithm used to obtain the following results was described in **Section 2.3** and written by Drs. Dennis Mackin and Jerimy Polf.

3.1.1. *OpenMP algorithm serial run*

The SOE algorithm uses iterations to progressively compute the most likely origins of the 100,000 cones that were measured by the CC during application of the proton beam. As more iterations are performed the results, or images, become more clearly defined. This convergence can be seen in **Figure 2**. Although at 100 iterations the image has some shape, it is clear that as the number of iterations increases this shape becomes more accurate. Additionally as the number of iterations increases the granularity of the results improve until the stopping point of 600 iterations whereby there is a distinct beam that can be seen.

The convergence in the algorithm happens, because with each iteration, the number of cones whose likely origin changes decreases. This means that as as the number of iterations increases, the amount of changes done to the overall histogram decreases. This behavior is quantified by the ratio of the number of changes to the total number of cones. The convergence of this ratio can be seen in **Figure 3** which shows log output of sample iterations output to stdout. From this, we can infer that the points that the program is estimating to be the points of origin for the prompt gamma emission are becoming more accurate. This would also mean that fewer changes are being made to the density matrix as more iterations are performed.

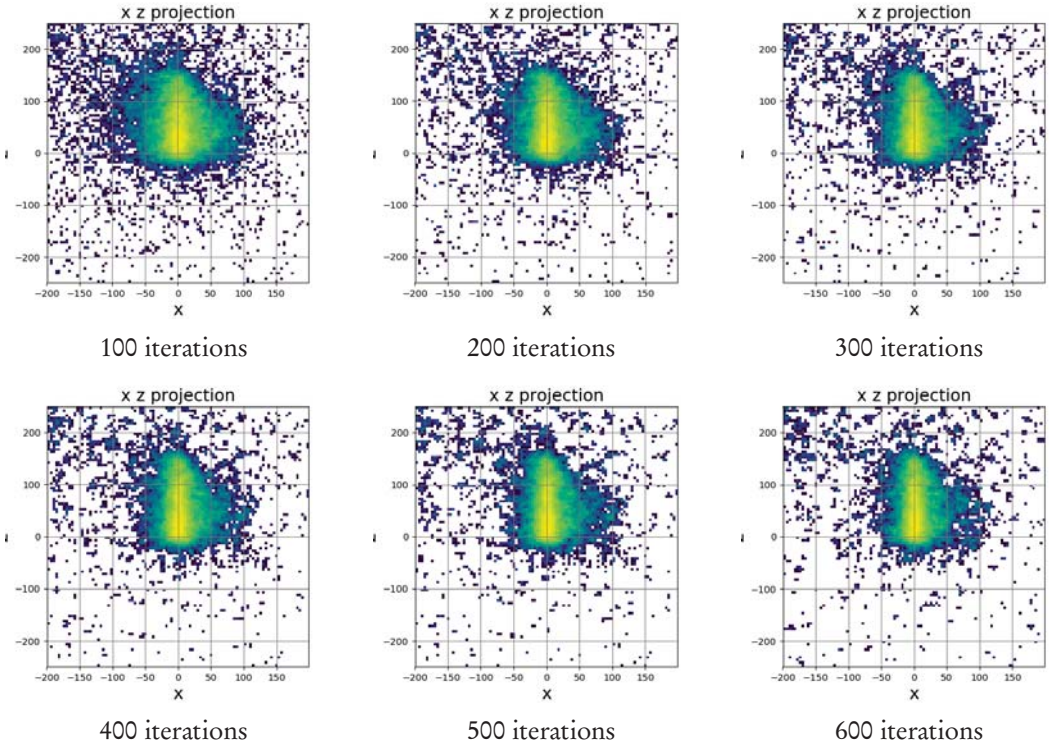

Figure 2. Reconstructed images computed by the OpenMP algorithm with 1 thread using Python post-processing up to 600 iterations

```
Iteration: 10, time 35, Number of Position Changes: 8799, ratio: 0.088
Iteration: 20, time 68, Number of Position Changes: 7485, ratio: 0.075
Iteration: 30, time 100, Number of Position Changes: 6498, ratio: 0.065
Iteration: 40, time 133, Number of Position Changes: 5784, ratio: 0.058
Iteration: 50, time 165, Number of Position Changes: 5339, ratio: 0.053
Iteration: 60, time 197, Number of Position Changes: 4971, ratio: 0.050
Iteration: 70, time 229, Number of Position Changes: 4469, ratio: 0.045
Iteration: 80, time 261, Number of Position Changes: 4336, ratio: 0.043
Iteration: 90, time 292, Number of Position Changes: 4119, ratio: 0.041
Iteration: 100, time 324, Number of Position Changes: 3944, ratio: 0.039
Iteration: 200, time 638, Number of Position Changes: 2990, ratio: 0.030
Iteration: 300, time 949, Number of Position Changes: 2684, ratio: 0.027
Iteration: 400, time 1257, Number of Position Changes: 2413, ratio: 0.024
Iteration: 500, time 1564, Number of Position Changes: 2195, ratio: 0.022
Iteration: 600, time 1870, Number of Position Changes: 2103, ratio: 0.021
--- Total Iterations: 600, time 1870,
Number of Position Changes: 2103, 100000, ratio: 0.021
Time Elapsed: 1884.54s
```

Figure 3. Iteration log output from the OpenMP algorithm with 1 thread.

At the end of the log output in **Figure 3**, the code records the observed wall clock time in the line denoted by "Time Elapsed". This is the time that we use later in the timing studies of the code.

It is worth noting that the images in **Figure 2** do not actually come from the same run of the code. This stems from the fact that the original code only outputs data for visualization at the final time. Hence, each plot in the figure is the final result of a run up to the specified number of iterations. It would be logical to say that if the 600 iteration run could have been post-processed at 500 iterations it should be the same as a 500 iteration run with the same parameters. This, however, is not the case because of the random number generator being used.

3.1.2. *OpenMP algorithm multi-threaded runs*

This code is designed to use OpenMP, which is an application programming interface that can be used on shared-memory multi-processor computers to allow for multi-threaded parallel processing. To maximize the speedup of the OpenMP algorithm it is necessary to use multiple threads. With OpenMP, memory cannot be pooled between nodes. Therefore, this algorithm only has the capability of using a single node at a time.

Figure 4 shows the results of iterations of a 2 thread run. The reconstructed images have shapes similar to those seen in **Figure 2**. The shapes of the beam are nearly indistinguishable and therefore acceptable results.

Similarly, the convergence behavior of the ratio for 2 threads in **Figure 5** follows the same pattern as **Figure 3**. That is, as the number of iterations increases the ratio decreases and the image become more refined and suitable in shape. However, small variations of results between **Figures 3** and **5** point to both the effect of differences in the random number sequences between runs and the slight differences possible between runs with different numbers of threads.

For our performance study, the code was run at 600 iterations on multiple threads ranging from 1 thread to 16 threads. It is important to note that even as the algorithm is run on more threads, the output image continues to be consistent with those obtained with serial runs.[6]

3.1.3. *OpenMP algorithm VTune results*

To initially understand the time inefficiency of the code, we used Intel's VTune profiling software to identify time intensive functions. The VTune Performance Characterization analysis identifies areas of OpenMP and/or MPI communication times as well as CPU and memory utilization. The Hotspots analysis was also used, which exhibits time intensive functions regardless of parallelism.

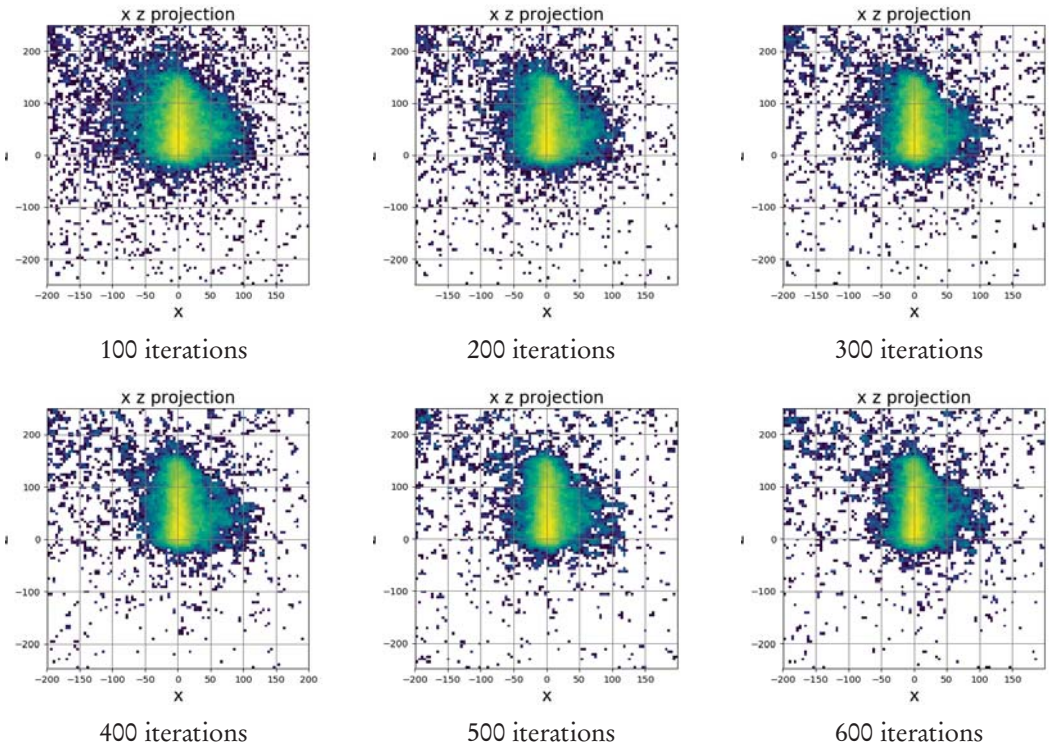

Figure 4. Reconstructed images computed by the OpenMP algorithm with 2 threads using Python post-processing up to 600 iterations.

Figure 6 shows VTune Performance Characterization for the OpenMP algorithm with 68 threads per node. Two functions are reported to have massive spin, or communication times, `kmp_wait_yield` and `kmp_barrier`, being 1838 seconds and 1521 seconds respectively. `kmp_barrier` and `kmp_wait_yield` are OpenMP library calls for communication between threads. These show us that while OpenMP may have optimized certain sections of the code, it ultimately led to longer run times due to communication times between threads. This spurred on the possibility of implementing MPI into the code to potentially cut these communication times down.

Figure 7 shows the VTune Hotspots Analysis with 68 threads per node. This type of analysis maps out the functions that are the most time intensive within the code without regards to communication times. We can see that the `getDensity`

```
Iteration: 10, time 14, Number of Position Changes: 8756, ratio: 0.088
Iteration: 20, time 27, Number of Position Changes: 7487, ratio: 0.075
Iteration: 30, time 39, Number of Position Changes: 6468, ratio: 0.065
Iteration: 40, time 51, Number of Position Changes: 5791, ratio: 0.058
Iteration: 50, time 63, Number of Position Changes: 5441, ratio: 0.054
Iteration: 60, time 74, Number of Position Changes: 5032, ratio: 0.050
Iteration: 70, time 86, Number of Position Changes: 4628, ratio: 0.046
Iteration: 80, time 97, Number of Position Changes: 4343, ratio: 0.043
Iteration: 90, time 109, Number of Position Changes: 4160, ratio: 0.042
Iteration: 100, time 120, Number of Position Changes: 3975, ratio: 0.040
Iteration: 200, time 231, Number of Position Changes: 3000, ratio: 0.030
Iteration: 300, time 338, Number of Position Changes: 2605, ratio: 0.026
Iteration: 400, time 444, Number of Position Changes: 2436, ratio: 0.024
Iteration: 500, time 548, Number of Position Changes: 2254, ratio: 0.023
Iteration: 600, time 652, Number of Position Changes: 2134, ratio: 0.021
--- Total Iterations: 600, time 652,
Number of Position Changes: 2134, 100000, ratio: 0.021
Time Elapsed: 661.26s
```

Figure 5. Iteration log output from the OpenMP algorithm using 2 threads up to 600 iterations.

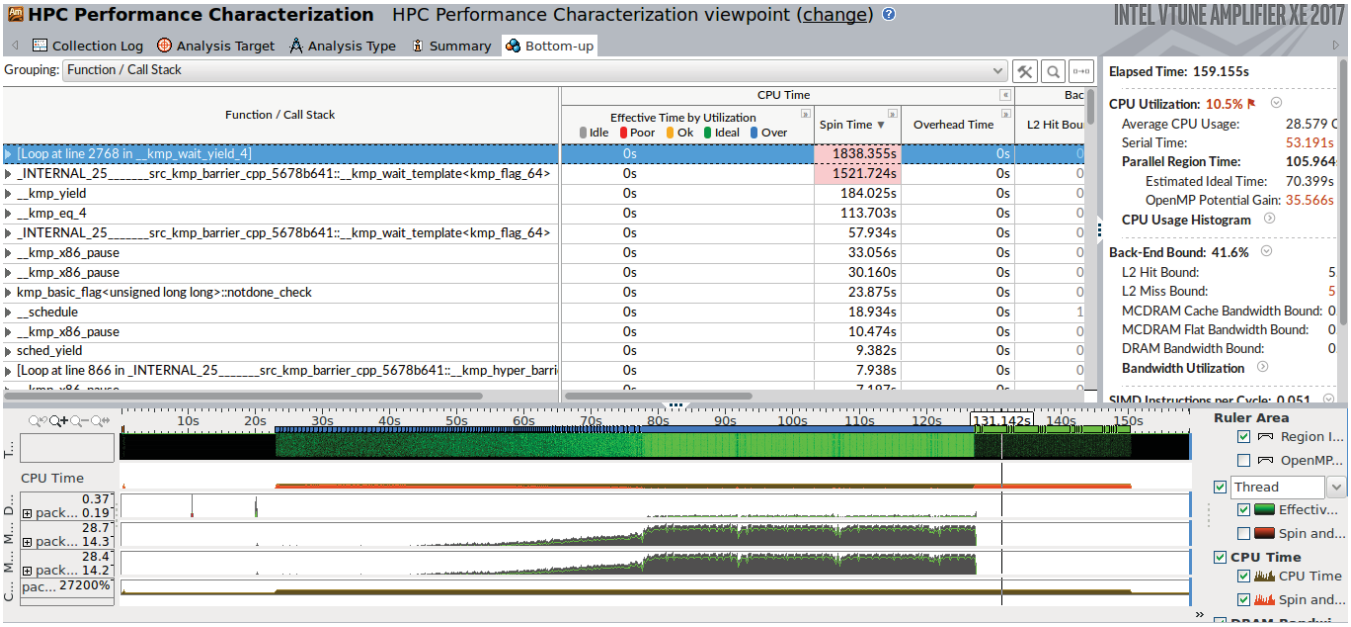

Figure 6. VTune Performance Characterization for the OpenMP algorithm with 68 threads per node.

function called from `DensityMatrix` is solely responsible for the majority of time use when the executable is run. When investigating the underlying code for `getDensity`, we quickly realized that the other three most time intensive functions were directly related and/or called from `getDensity`. For example, `getBinNumber`, and the `ASHDensity::getDensity`, the second and fourth most time intensive function, are directly called from the `getDensity` function. This is a logical process because the `DensityMatrix` object's `getDensity` function calls `ASHDensity` object's `getDensity` which also calls their `getBinNumber` method. So this cascading spin time is a direct result of all the threads chasing down several sets of nested pointers in C++. The fourth time intensive function is the `updateMatrix` function. This function's impact is the result of a `critical` pragma that wraps around it.

Both analysis types showed time critical areas to focus our attention on. The Performance Characterization results clearly showed that OpenMP library calls were costing massive wait times in order for threads to synchronize, while the Hotspots Analysis showed functions that could potentially benefit from parallelization. With these results in hand, a clear course of action could be mapped out.

3.2. *Modified MPI algorithm*

As detailed in **Sections 2.4** and **2.5**, the MPI algorithm is different from the OpenMP algorithm in that the histogram is updated at the end of each iteration, not after updating each cone. This has the potential for causing slower convergence, and we therefore report studies with twice as many iterations than used for the OpenMP studies in the following. But the advantages of the MPI algorithms are two-fold: (i) Parallelism is not restricted to one node any more, but can be extended to any number of parallel nodes available, and (ii) speedup is not limited any more if progressively more nodes can be used in parallel. These two-fold advantages are the goal of both MPI algorithms.

3.2.1. *Modified MPI algorithm serial run*

A second, modified MPI algorithm is described in **Section 2.5** and reflects the observation that the major cost of parallelism with MPI is the cost of communication. For the original MPI algorithm, this cost amounts to a call to the communication command `MPI_Allreduce` every 1 iteration. The modified MPI algorithm decreases this cost by communicating only every 10 iterations. The major concern with this algorithm is possible further degradation of the convergence behavior. With the processes only having access to a histogram that was developed 10 iterations prior to their current iteration there is

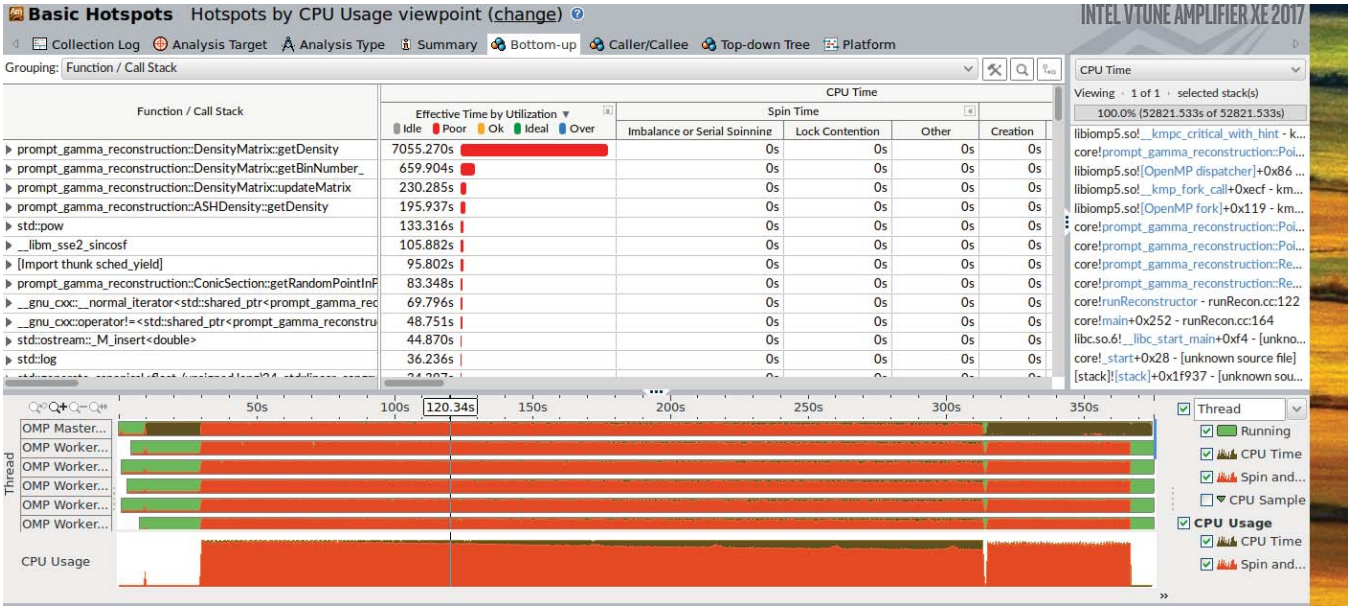

Figure 7. VTune Hotspots Analysis for the OpenMP algorithm with 68 threads per node.

a possibility that the lack of updates causes the images to degrade to unusable quality. For the modified MPI algorithm in serial, **Figure 8** starts out with a rough cloud of points which form into a wider beam around the 400 iteration mark. The beam starts to narrow and become more defined at around 800 iterations. After that, the images remain similar to previous images. Visually the convergence can be seen from this image set, starting out with a very rough image and going to something much more refined and recognizable. The modified MPI algorithm in serial shows the same behavior as the original MPI algorithm[6] and shows only slightly slower convergence than the original OpenMP code in **Figure 2**.

Furthermore, the log output in **Figure 9** for the modified serial run shows that the ratio is a little higher than the OpenMP algorithm, but the general behavior of convergence remains similar.

We note that the images in **Figure 8** are produced by Matlab instead of Python post-processing. As discussed in **Section 2.4**, this change gains the advantage that one run of the code now outputs in steps of 100 iterations, thus all images in the figures from MPI algorithms come from the same run.

3.2.2. *Modified MPI algorithm multi-process runs*

Figure 10 shows some minor image degradation again in the first images, compared to the original OpenMP algorithm, but is apparently identical to **Figure 8** for the serial run. As in **Figure 8**, the cloud starts out similar to **Figure 2** but persists for a couple hundred iterations beyond the first image. However, by 700 or 800 iterations the beam is well formed, albeit slightly wider than the original MPI.[6] The images visually converge at around 900 iterations, which coincides with the log file output in **Figure 11**. This slower convergence behavior can be more clearly demonstrated comparing the modified MPI algorithm log output in **Figure 11** to the multi-threaded OpenMP **Figure 5**. We might recommend to use a slightly larger number of iterations in production runs, such as 700 or 800 iterations instead of the originally used 600 for the OpenMP algorithm.

3.2.3. *MPI VTune*

To gauge the efficiency of the new MPI implemented algorithm, the code was profiled once more with Intel's VTune software. We used the same analysis specifications to determine if communication times were indeed faster than the OpenMP algorithm, as well as watching our previous time intensive functions.

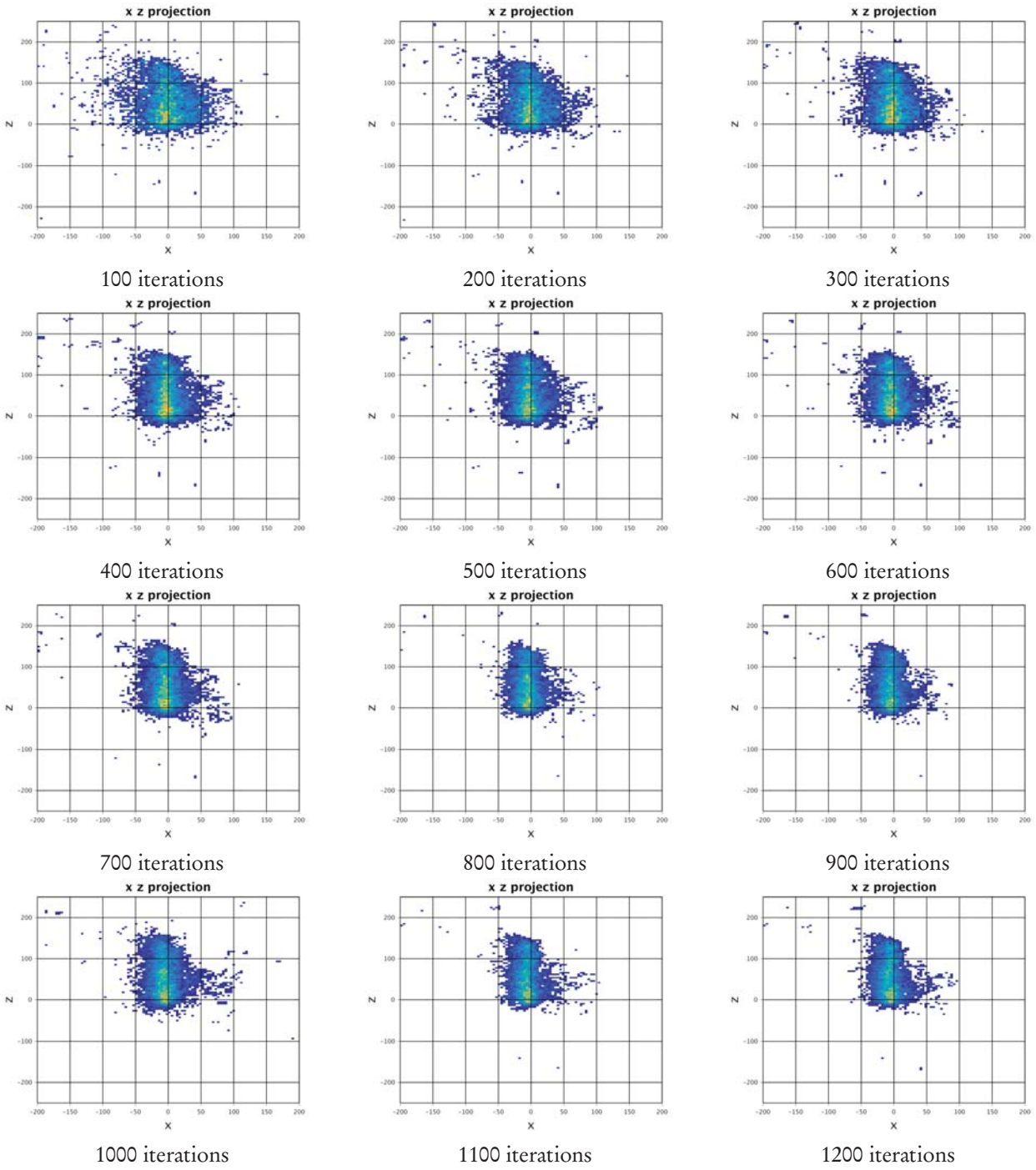

Figure 8. Reconstructed images computed by the modified MPI algorithm with 1 process up to 1200 iterations using Matlab post-processing.

Figure 12 shows the VTune Performance Characterization of the modified MPI algorithm with 4 processes per node. Implementing MPI did indeed improve the communication times, or 'spin' far greater than expected. The first analysis showed that OpenMP communication took a staggering 1838 seconds, while our MPI algorithm had a maximum communication time of only 0.130 seconds. This affirmed our decision to introduce MPI into the algorithm.

Figure 13 shows the VTune Hotspots Analysis for the same modified MPI algorithm with 4 processes per node. This Hotspots Analysis produced similar results to the previous run. While `getDensity` and its related function calls were still

```
Iteration: 10, time 18, Number of Position Changes: 18815, ratio: 0.188
Iteration: 20, time 34, Number of Position Changes: 19761, ratio: 0.198
Iteration: 30, time 50, Number of Position Changes: 16207, ratio: 0.162
Iteration: 40, time 66, Number of Position Changes: 13412, ratio: 0.134
Iteration: 50, time 82, Number of Position Changes: 11338, ratio: 0.113
Iteration: 60, time 98, Number of Position Changes: 9841, ratio: 0.098
Iteration: 70, time 114, Number of Position Changes: 8835, ratio: 0.088
Iteration: 80, time 129, Number of Position Changes: 7675, ratio: 0.077
Iteration: 90, time 145, Number of Position Changes: 7198, ratio: 0.072
Iteration: 100, time 161, Number of Position Changes: 6655, ratio: 0.067
Iteration: 200, time 315, Number of Position Changes: 4479, ratio: 0.045
Iteration: 300, time 466, Number of Position Changes: 3821, ratio: 0.038
Iteration: 400, time 644, Number of Position Changes: 3390, ratio: 0.034
Iteration: 500, time 893, Number of Position Changes: 3146, ratio: 0.031
Iteration: 600, time 1139, Number of Position Changes: 3018, ratio: 0.030
Iteration: 700, time 1384, Number of Position Changes: 2889, ratio: 0.029
Iteration: 800, time 1629, Number of Position Changes: 2837, ratio: 0.028
Iteration: 900, time 1873, Number of Position Changes: 2769, ratio: 0.028
Iteration: 1000, time 2116, Number of Position Changes: 2688, ratio: 0.027
--- Total Iterations: 1200, time 2598,
Number of Position Changes: 2688, 100000, ratio: 0.027
Time Elapsed:  2610s
```

Figure 9. Iteration log output from the modified MPI algorithm using 1 processes up to 1200 iterations.

responsible for being the most time critical calls, the parallelism imposed onto these helped to reduce the footprint. The introduction of MPI eliminated the waiting associated with `updateMatrix` but did not smoothly allow the elimination of the nested object calls associated with `getDensity`. Converting more C++ object code into C code would allow `getDensity` to be made much for efficient or removed altogether.

3.3. *Performance studies*

To understand the impact of the changes we implemented on the run time, a study was created to compare the performance of the original OpenMP algorithm, our (original) MPI algorithm, and the modified MPI algorithm. **Table 1** shows the timing results of our study. Note that the performance studies used 600 iterations for all algorithms to provide a direct comparison of the times.

The first studies ran were to determine the performance of the OpenMP algorithm shown in the first row of timings in **Table 1**. The code was tested when run on one node using 1, 2, 4, 8, and 16 threads to get an idea of the speedup. With 1 thread, the code ran a staggering 1885 seconds, or roughly 30 minutes. As the number of threads increased, the run times gained significant speedup as had been expected. For example, at 2, 4, and 8 threads, the run times had been reduced by more than fifty percent each time. While still improving at 16 threads, times decreasing from 188 seconds to 105 seconds, is not the same rate of improvement as can be observed in the first 4 increments. This speed of 105 seconds is the best possible run time observed for this algorithm, since OpenMP is limited to one node; runs for 32 and 64 cores are marked as N/A in the table.

The first changes to the code allowed for the implementation of MPI and disabled all OpenMP pragmas. These adjustments allowed for both the use of distributed memory and multiple processes across nodes for each job. In order to assess the benefits of MPI, tests were run using numbers of processes that mirror the number of threads in the previous study. That is, the studies in each row of timings in **Table 1** the same hardware cores in the CPUs on one node; beyond 16 processes, MPI uses more nodes and thus more hardware, while OpenMP cannot be utilized beyond one node. Already the performance of our original MPI algorithm from **Section 2.4** saw improvement, bringing the run time to 1592 seconds for one process due to other improvements of the code. At 2 processes, the time dropped by roughly a third down to 546 seconds, similar to the speedup seen with OpenMP. For the rest of the runs, from 8 to 64 processes, the code did not speed up as much as had been expected, reaching its fastest time at 354 seconds for 8 processes and rising to 430 seconds at 64 processes. This

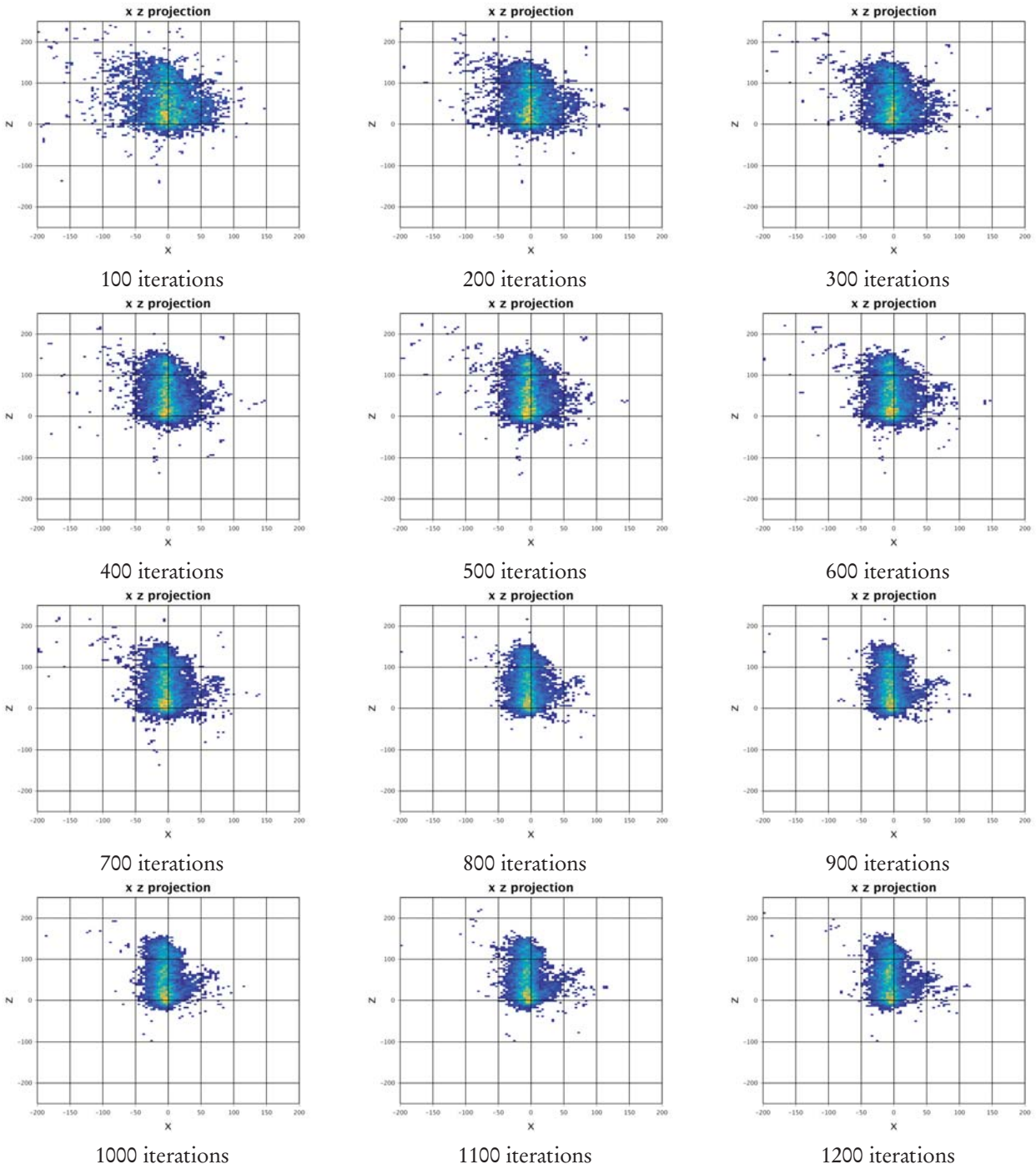

Figure 10. Reconstructed images computed by the modified MPI algorithm with 2 processes up to 1200 iterations using Matlab post-processing.

exhibits that parallel communications eventually overwhelm the increased efficiency of splitting up the computational work between processes.

In the modified MPI algorithm, the histogram would be updated every 10 iterations as described in **Section 2.5**. This change allowed for a significant speedup. At one process, the algorithm fully ran in 985 seconds, almost half of that for the OpenMP with one thread, due to additional improvements in the code. The increases in processes showed reduction in run times, ending on 64 processes with 83 seconds.

```
Iteration: 10, time 11, Number of Position Changes: 18727, ratio: 0.187
Iteration: 20, time 19, Number of Position Changes: 19703, ratio: 0.197
Iteration: 30, time 27, Number of Position Changes: 16209, ratio: 0.162
Iteration: 40, time 35, Number of Position Changes: 13374, ratio: 0.134
Iteration: 50, time 43, Number of Position Changes: 11165, ratio: 0.112
Iteration: 60, time 52, Number of Position Changes: 9851, ratio: 0.099
Iteration: 70, time 60, Number of Position Changes: 8658, ratio: 0.087
Iteration: 80, time 67, Number of Position Changes: 7696, ratio: 0.077
Iteration: 90, time 75, Number of Position Changes: 7139, ratio: 0.071
Iteration: 100, time 84, Number of Position Changes: 6783, ratio: 0.068
Iteration: 200, time 162, Number of Position Changes: 4493, ratio: 0.045
Iteration: 300, time 240, Number of Position Changes: 3858, ratio: 0.039
Iteration: 400, time 316, Number of Position Changes: 3493, ratio: 0.035
Iteration: 500, time 392, Number of Position Changes: 3081, ratio: 0.031
Iteration: 600, time 468, Number of Position Changes: 2936, ratio: 0.029
Iteration: 700, time 543, Number of Position Changes: 2874, ratio: 0.029
Iteration: 800, time 618, Number of Position Changes: 2748, ratio: 0.027
Iteration: 900, time 692, Number of Position Changes: 2677, ratio: 0.027
Iteration: 1000, time 767, Number of Position Changes: 2651, ratio: 0.027
--- Total Iterations: 1200, time 915,
Number of Position Changes: 2651, 100000, ratio: 0.027
Time Elapsed:   928s
```

Figure 11. Iteration log output from the modified MPI algorithm using 2 processes up to 1200 iterations.

4. CONCLUSIONS

The original code provided by Dr. Polf and Dr. Mackin implements an algorithm using the shared-memory parallel library OpenMP, which is constrained to all cores of 1 node which limits performance. In order to see a significant speedup, this code needed to given the ability to run on multiple nodes. In order to have this capability, the algorithm was modified so that it could be run using the distributed-memory parallel communication library MPI. Modifications to the algorithm included distributing the work associated with the large number of cones in each iteration to the parallel processes. Each process works on a section of the total number of cones, thus the work is distributed. The first version of the MPI algorithm updates the global histogram updated after every iteration.[6] This was changed in the modified MPI algorithm to allow for

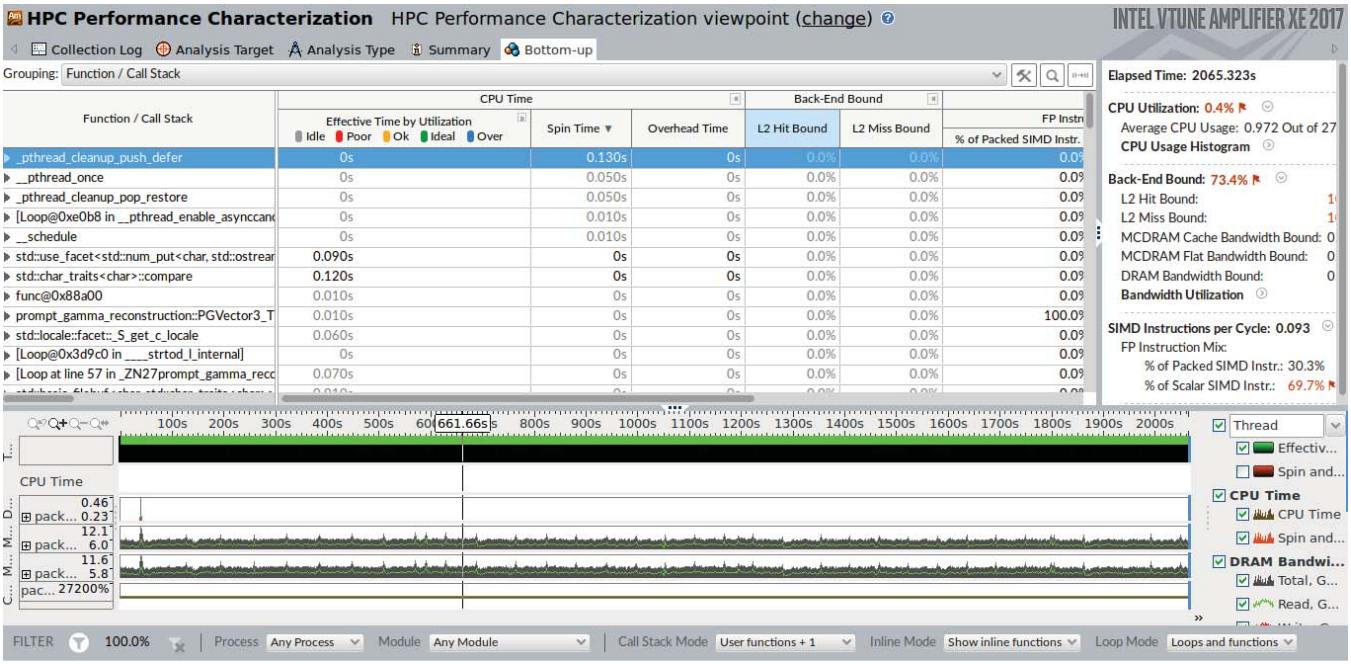

Figure 12. VTune Performance Characterization for the Modified MPI algorithm with 4 processes per node.

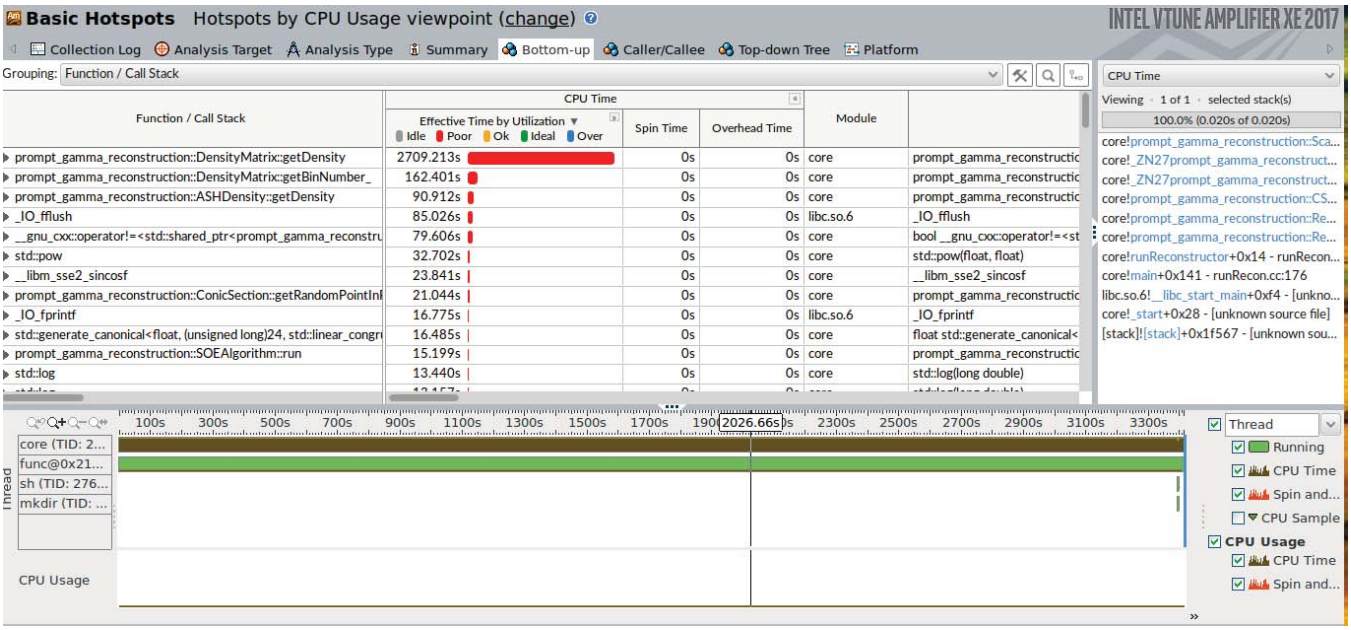

Figure 13. VTune Hotspots Analysis for the Modified MPI algorithm with 4 processes per node.

further speedup by only updating the histogram every 10 iterations. Various code improvements helped already improve the serial time from 1885 seconds to 985 seconds. In parallel, OpenMP provided a run time of 105 seconds on 1 node. By implementing an algorithm designed to use MPI, we were able to move beyond 1 node and obtain the best run time of 85 seconds.

By implementing MPI in this algorithm, this study has given the algorithm potential for further speedup. MPI's distributed memory and multiple-processing power has been shown to be capable to scale down run times. For these reasons, the algorithm developed here has great potential to be sped up as necessary to be used in a clinical setting with more code improvements and with the use of hybrid MPI+OpenMP, which we did not explore yet. In particular, the formulation lays the groundwork to be used on the brand new many-core Intel Xeon Phi KNL processor with 64+ computational cores, since it is demonstrated that pure OpenMP parallelism is not optimal on that hardware.

Computational cores	1	2	4	8	16	32	64
OpenMP multi-threading	1885	661	344	188	105	N/A	N/A
Original MPI algorithm	1569	546	372	354	511	477	430
Modified MPI algorithm	985	480	277	194	147	113	83

Table 1. Observed wall clock time in seconds for reconstruction with 600 iterations.

ACKNOWLEDGEMENTS

These results were obtained in the REU Site: Interdisciplinary Program in High Performance Computing in the Department of Mathematics and Statistics at the University of Maryland, Baltimore County (UMBC) in Summer 2017 (hpcreu.umbc.edu). This program is funded by the National Science Foundation (NSF), the National Security Agency (NSA), and the Department of Defense (DOD), with additional support from UMBC, the Department of Mathematics and Statistics, the Center for Interdisciplinary Research and Consulting (CIRC), and the UMBC High Performance Computing Facility (HPCF). HPCF is supported by the U.S. National Science Foundation through the MRI program (grant nos. CNS–0821258 and CNS–1228778) and the SCREMS program (grant no. DMS–0821311), with additional substantial support from UMBC. Co-author James Della-Giustina was supported in part, by the Math Computer Inspired Scholars program, through funding

from the National Science Foundation and also the Constellation STEM Scholars Program, funded by Constellation Energy. Co-authors Johnlemuel Casilag and Aniebiet Jacob were supported, in part, by the UMBC National Security Agency (NSA) Scholars Program through a contract with the NSA. The research reported in this publication was supported by the National Institutes of Health National Cancer Institute under award number R01CA187416. The content is solely the responsibility of the authors and does not necessarily represent the official views of the National Institutes of Health. We acknowledge the Texas Advanced Computing Center (TACC) at The University of Texas at Austin for providing HPC resources that have contributed to the research results reported within this paper.

REFERENCES

1. Dennis Mackin, Steve Peterson, Sam Beddar, and Jerimy Polf. (2012) Evaluation of a stochastic reconstruction algorithm for use in Compton camera imaging and beam range verification from secondary gamma emission during proton therapy. *Phys. Med. Biol.*, 57:3537–3553.
2. Jerimy C. Polf and Katia Parodi. (2015) Imaging particle beams for cancer treatment. *Physics Today*, 68(10):28–33.
3. Fernando X. Avila-Soto, Alec N. Beri, Eric Valenzuela, Abenezer Wudenhe, Ari Rapkin Blenkhorn, Jonathan S. Graf, Samuel Khuvis, Matthias K. Gobbert, and Jerimy Polf. (2015) Parallelization for fast image reconstruction using the stochastic origin ensemble method for proton beam therapy. Technical Report HPCF–2015–27, UMBC High Performance Computing Facility, University of Maryland, Baltimore County.
4. Andriy Andreyev, Arkadiusz Sitek, and Anna Celleri. (2011) Fast image reconstruction for Compton camera using stochastic origin ensemble approach. *Med. Phys.*, 38:429-435.
5. Intel Developer Zone. Intel VTune Amplifier. Documentation at the URL: *https://software.intel.com/en-us/intel-vtune-amplifier-xe-support/documentation* (accessed January 2018).
6. Johnlemuel Casilag, James Della-Giustina, Elizabeth Gregorio, Aniebet Jacob, Carlos Barajas, Matthias K. Gobbert, Dennis S. Mackin, and Jerimy Polf. (2017) Development of fast reconstruction techniques for prompt gamma imaging during proton radiotherapy. Technical Report HPCF–2017–16, UMBC High Performance Computing Facility, University of Maryland, Baltimore County.

ABOUT THE STUDENT AUTHORS

Johnlemuel Casilag and Aniebiet Jacobs will graduate in May 2020, both with a B.S. in computer science from University of Maryland, Baltimore. John plans on pursuing an advanced technical degree in artificial intelligence. Elizabeth Gregorio will graduate from Hamline University in May 2018 with a B.S. in Physics. After graduation she hopes to continue her education studying computational fluid dynamics. James Della-Giustina will graduate in December 2019 with a B.S. in computer science and plans to work with embedded systems.

PRESS SUMMARY

Proton beam radiation treatment has the potential to greatly reduce the amount of healthy tissue that receives radiation during treatment for cancerous tumors as opposed to x-ray radiation treatment. This paper focuses on improving performance for prompt gamma imaging software that would allow physicians to monitor the dose delivered in real time on the operating table, a tool that currently does not exist. With the implementation of the parallel computing library MPI, we increased the speed of the code as well as laid the foundation for further performance improvements to provide physicians with this much needed advantage.

Knowledge and Behaviors Associated with a Campus Tobacco-Free Policy

Sarah Powell[a], Cassie Odahowski[b,c], Elizabeth Crouch[d], Erica Sercy[b,c], Jackie Knight[e], & Jan M. Eberth[b,c]*

[a] *Department of Epidemiology and Biostatistics, College of Public Health, University of South Florida, Tampa, FL*
[b] *Department of Epidemiology and Biostatistics, Arnold School of Public Health, University of South Carolina, Columbia, SC*
[c] *Statewide Cancer Prevention and Control Program, Arnold School of Public Health, University of South Carolina, Columbia, SC*
[d] *Department of Health Services Policy and Management, Arnold School of Public Health, University of South Carolina, Columbia, SC*
[e] *Healthy Carolina Coalition, University of South Carolina, Columbia, SC*

*Student: sepowell1@health.usf.edu **
Mentor: jmeberth@mailbox.sc.edu

ABSTRACT
Objective: Nearly half of U.S. colleges/universities have implemented tobacco-free campus policies. This study analyzed knowledge, attitudes, and practices associated with the tobacco-free policy at a large public university. It is important to study public university tobacco policies to determine the most efficient and cost-effective way to reduce tobacco related disease due to tobacco use and exposure.
Methods: This study used a cross-sectional, campus-wide electronic survey distributed in November 2016. The primary outcomes of interest included 1) correct knowledge of the tobacco-free policy, 2) community member willingness to approach observed violation of the policy, and 3) a positive opinion of the policy's effectiveness. Descriptive statistics and logistic regression were used to examine the impact of demographic factors on the outcomes.
Results: After analysis, the team found that 23% of university faculty, staff, and students had incorrect knowledge about the campus tobacco-free policy. Almost 70% of the university community reported not having approached a smoking violator. Males were significantly less likely to understand the tobacco-free policy in full, approach a violator, or have a positive opinion about its effectiveness. Staff had better knowledge of the policy, a higher likelihood of approaching a violator, and a better opinion about the policy's effectiveness compared to graduate and undergraduate students.
Conclusions: Interventions are needed to increase awareness and confidence regarding implementation and enforcement of the tobacco-free policy on campus, particularly among faculty and students. This paper expands on the currently increasing knowledge of tobacco-free policy enforcement and benefits.

KEYWORDS
Campus; Tobacco Regulation; Tobacco; Secondhand Smoke; Cross-Sectional Survey

INTRODUCTION

Environmental tobacco exposure (ETS) research has demonstrated the public health externalities to second hand smoke.[1,2] Exposure to second hand smoke increases the risk of lung cancer, heart disease, and respiratory symptoms and illnesses for nonsmokers.[3] E-cigarettes are often included in tobacco-free policies as well because they still contain nicotine, which could possibly lead to future tobacco use in other forms, such as cigarettes.[4] All of these increased risks have led to tobacco-free policies in numerous public settings, including universities.[5] Between 2011 and 2017, the proportion of 2- and 4- year public and private colleges and universities that had implemented 100% tobacco-free policies increased by more than 300%.[6]

Previous research has demonstrated the effectiveness of tobacco-free campuses in reducing tobacco use and changing smoking behavior.[7-9] Most students, faculty and staff report that they have been exposed to second hand smoke on campus;[10-14] many of these individuals report that they believe this exposure is harmful and that the university has a responsibility to curb secondhand smoke exposure via campus tobacco-free policies.[12,13,15] The purpose of tobacco-free policies is two-fold: the bans decrease ETS but also de-normalize smoking as a socially acceptable behavior.[16] This is especially important for young adults, who have the highest smoking rate of any age group in the United States and who are targeted by tobacco industry advertising.[17,18] Self-reported smoking rates among college students range from 9% to 25%, with rates in the United States being the highest among universities in the South.[10,11,15,19]

Smoking prevention efforts such as tobacco-free policies can lead to the shifting of social norms regarding tobacco use, which include socially acceptable practices.[20] Formal policies, such as tobacco-free policies on college campuses, can enforce new behaviors through stigmatizing smoking.[21] Tobacco bans stigmatize spaces, increasing the segregation of smoker and non-

smokers.[22] Stigmatizing smokers may have positive results by increasing the level of social unacceptability and the acceptability of tobacco-free policy enforcement.[21,23] This may be critical for young adults, for whom the initiation of smoking may not fully take hold for several years.[24]

A nationally representative survey of 4-year colleges and universities in the United States showed broad support (over 75%) for tobacco-free campus policies regardless of smoking status.[25] Other smaller studies have reflected this level of support, although current smoking status tends to reduce support and female gender consistently increases support.[10-15,19] Longitudinal studies on the impact of smoke-free campus policies have found mixed but generally positive results: one found significantly reduced smoking behavior among students on a campus with a smoke-free policy,[8] another found that strict enforcement of the policy increased policy compliance,[26] and a third found that although the policy was not effective at reducing general smoking prevalence among students, it did reduce self-reported second hand smoke exposure on campus.[9]

Few studies have examined the enforcement of tobacco-free policies on college campuses.[26] None have focused exclusively on the influence, compliance, or enforcement of a tobacco free campus in the Southern portion of the United States, where young adults are more likely to be heavy smokers than their counterparts in other regions of the country.[27] The purpose of this study was to analyze knowledge, attitudes, and practices associated with the tobacco-free policy at a large public university in South Carolina.

MATERIALS AND METHODS

Context

Following the American College Health Association's 2009 recommendation for all colleges and universities to implement a tobacco-free campus policy,[28] the University of South Carolina (USC) in Columbia, SC implemented a campus-wide ban on all tobacco products (including e-cigarettes) on January 1, 2014.[29,30] Prior to the campus-wide ban, numerous policies that limited smoking at specific locations were in place, discouraging tobacco use on university property. Specifically, tobacco use was explicitly prohibited within 25 feet of university-owned and -leased buildings, vehicles, and equipment operated other than vehicles.[29,31]

The policy was announced on the university website,[31] references to the policy were added to student handbooks, and signs were posted conspicuously around campus on buildings, trashcans, and posts along walking paths. A Tobacco Free Task Force, comprised of USC students, staff, and faculty, worked to craft, finalize, and promote the campus-wide tobacco ban in partnership with Healthy Carolina, a part of the campus health system.[29,31]

The Tobacco Free Task Force assigned the enforcement of the tobacco-free policy to the Carolina community, which consists of students, faculty, staff, and volunteers, rather than university police or security.[29,31] Enforcement consists of volunteers bringing the smoking policy infraction to the attention of the person(s) committing the violations.[29] If the person(s) violating the policy does not respond to this reminder, then the student, faculty, staff, and/or volunteer may report the violation to five different entities on campus: the Office of Student Conduct, the Office of Business Affairs, law enforcement, and/or the violator's unit head, immediate supervisor, or director, depending on who is reporting and who is committing the violation.[31] Various citations can be handed to the violator by these entities. If the person wants to quit smoking, he/she can be referred to tobacco cessation services through USC.[32] If there is no intent to quit and verbal reminders are ignored, there are a range of possible consequences, including a written report kept on record for students, a $50 fine, a report to a supervisor (faculty, staff, contractors, and vendors), or law enforcement involvement (campus visitors).[31] After the enactment of this policy in 2014, there were continued reports and sightings of tobacco use on campus. A NCHA assessment in 2012 resulted in 68% of the student body at the time supporting the current tobacco-free policy and staff assessments conducted in 2011 found 84.9% of faculty/staff support the current tobacco-free policy.[28] Providing evidence of the overall appeal the current tobacco-free policy has to faculty/staff, and students.

This study used a cross-sectional, campus-wide electronic survey distributed in November 2015. A web-based survey (thereafter referred to as the Healthy Carolina Survey) consisting of 25 items related to the campus tobacco-free policy was distributed to all USC faculty, staff, and students via an email invitation from the university president and Healthy Carolina. The survey was based off a tobacco-free policy survey used in the past by Florida State University, which was credited as a reliable survey regarding the current tobacco-free policy. Florida State University has the same tobacco-free policy as the University of South Carolina, which includes the ban of all forms of tobacco including e-cigarettes. The survey was only open to participants who had a valid University of South Carolina email address. There were controls in place to ensure that the survey was only taken once per email address to offset the possibility of participants taking the survey more than once. One reminder was sent out on November 17, 2015. The survey was available from November 2, 2015 to December 6, 2015. To encourage survey completion, incentives of various amounts, including gift cards, school event tickets, and other miscellaneous items, were provided to a limited number of respondents. The winners of incentives were randomly drawn from completed surveys.

Variable	Survey Participants N (%)
Status	
Freshman	870 (14.7)
Sophomore	823 (13.9)
Junior	852 (14.4)
Senior	977 (16.5)
Graduate Student	941 (15.9)
Staff	1,030 (17.4)
Faculty	427 (7.2)
Gender	
Male	2,089 (40.4)
Female	2,935 (56.7)
Transgender	26 (0.5)
Prefer Not to Respond	125 (2.4)
Race/Ethnicity	
African American	270 (8.6)
American Indian or Alaskan	29 (0.9)
Asian or Pacific Islander	120 (3.8)
Hispanic or Latino	88 (2.8)
White	2,494 (79.8)
Other	125 (4.0)

Table 1. Demographics of Healthy Carolina Survey Participants *(N=5,920)*
Note: Number of responses varies per question and may not equal the full sample size. Proportions reported based on sample size for each respective question.

Measures
The school in 2015 had 39,995 faculty, staff, and students (freshman, sophomores, juniors, seniors, graduates, medical school, pharmacy school, and law school) combined. All 39,995 had University of South Carolina email addresses and received invitations to complete surveys. Once the survey ended the total sample size N=6876, which did not account for missing data. Once missing data for question 4, which asked if participants knew current tobacco-free policy, and question 8, which asked how many days participants were exposed to second hand smoke were removed, N=5504 observations. When the missing data for gender, race or status are removed N=2916 observations.
We defined a respondent as having accurate knowledge about the campus tobacco-free policy if he/she chose the responses that described the current policy (N=5771), namely "The use of all tobacco products are prohibited on all campus property" and "[Yes], electronic cigarettes are considered a tobacco product and thereby prohibited by the university's tobacco-free policy". Confidence/experience approaching violators was defined as respondents who stated, "[Yes], since January 1, 2014, I have informed a person using a cigarette, cigar, pipe, smokeless tobacco, hookah, or an electronic cigarette on campus that the use of these products is prohibited." A positive opinion of the tobacco-free policy was defined as "[Yes], I feel the university's tobacco-free policy has reduced the use of tobacco and tobacco-derived products on the Columbia campus."

Data Analysis
Descriptive statistics were produced from de-identified survey data for respondent demographics, as well as survey responses. Multiple logistic regression models were used to examine the association of respondent characteristics (gender, class or employment status, and race) with three separate outcomes: accurate knowledge about the campus tobacco-free policy,

confidence/experience approaching violators, and positive opinion of the tobacco-free policy effectiveness. Covariate categories were collapsed as necessary to ensure valid estimates. Statistical significance was based on a 0.05 alpha level. All analyses were performed using SAS Version 9.3 (SAS Institute, Cary, NC).

Human Subjects Approval Statement
Prior to data collection, the USC Institutional Review Board reviewed and deemed the study protocol for this project as exempt (Pro00044066).

RESULTS
The Healthy Carolina Survey had N=6876 respondents with a complete or partially complete data, equivalent to approximately 17% of the University of South Carolina community. The response rate was evenly distributed between faculty, staff, and students based on the University of South Carolina population (**Table 1**). There was a slight over-representation of graduate students and upper undergraduates (junior and senior) in comparison to lower undergraduates (sophomore and freshman). Staff and males were also slightly over-represented.

Although 77% of the respondents correctly identified the current tobacco-free policy, only 47.7% of respondents understood the policy in full. Understanding the policy in full was measured by correctly identifying "the use of all tobacco products are prohibited on all campus property", and that e-cigarettes were included in the policy. In total, 44.1% of respondents answered incorrectly when asked if e-cigarettes were included in the policy (i.e., an incorrect answer was either answering that e-cigarettes are not included in the policy or not knowing whether they are included). When asked about e-cigarette use observed 30 days prior to the survey, 59.6% of respondents answered they had seen e-cigarette use at least one day during that period. Survey results also revealed that 93.5% of people have observed tobacco being smoked on campus within the 30 days prior to the survey; thus, nearly all respondents had the opportunity to approach a violator in the past month.

Perceived enforcement of the policy was low among students (22.5%) and faculty/staff (32.5%). Only 18.7% of participants reported having approached a violator of the tobacco-free policy. Of those respondents who had approached a violator (n=1,003), 12.8% reported that the violator did stop their tobacco use after being approached, 11.3% said the violator moved to off-campus property, 52.5% said the violator did not stop their tobacco use, and 23.5% said they were unsure about the outcome of approaching the violator. The respondents who did not approach a violator (n=3,703) were asked why they did not and what might make them more comfortable doing so. Survey responders were allowed to select more than one answer on the survey question. The most common selected answers for not approaching a violator were not feeling comfortable (55.2%), not feeling like they possessed the authority (40.9%), and feeling like they would upset the person (32.2%). There was also the option to write-in answers, which n=1,111 survey respondents did.(30%). The respondents indicated that seeing more signage about the policy, knowing more about consequences of the policy, and observing others enforcing the policy would increase their comfort in approaching violators. Some respondents also wrote in answers to this survey question as well (n=1319). The corrective actions for tobacco violations were not well known among respondents, with only 46.4% knowing the consequences of policy violations. Although perceived enforcement is low (22.5-23.5%, **Table 2**), 69.5% of persons surveyed believe tobacco use has declined on campus since the tobacco-free campus policy was enacted.

Results from multiple logistic regression models revealed associations between in student/employment status, gender, and race for all three outcomes modeled (**Table 3**). University staff were significantly more likely than faculty, graduate students, or undergraduates to correctly identify the current campus tobacco policy, including inclusion of e-cigarettes in the policy. They were also more likely to have approached a violator and have a positive opinion of the policy's effectiveness, particularly compared to undergraduate and graduate students. Despite having fewer respondents with accurate knowledge about the tobacco-free policy and less experience approaching violators than their staff counterparts, faculty were significantly more likely to feel the policy was working well. Compared to females, males were significantly less likely to have an accurate knowledge of the policy in full, have experience approaching a violator, or feel positively about the policy's effectiveness. Minority members of the USC community were more likely than their white counterparts to have intervened on an observed smoking violation, but were not significantly different in terms of their knowledge level or opinion about the policy's effectiveness.

Survey Item	Response N (%)
Participant correctly identified current tobacco policy	
Yes	4,446 (77.0)
No	1,325 (23.0)
Electronic cigarettes are considered a tobacco product and thereby prohibited by the University's tobacco-free policy	
Yes	3,075 (55.9)
No	628 (11.4)
I Don't Know	1,801 (32.7)
The tobacco policy is being enforced by *students* on campus	
Agree	1,212 (22.5)
Disagree	4,176 (77.5)
The tobacco policy is being enforced by *faculty and staff* on campus	
Agree	1,753 (32.5)
Disagree	3,635 (67.5)
Informed a person violating the tobacco policy on campus that the use of tobacco products is prohibited	
Yes	1,003 (18.7)
No	3,730 (69.6)
Have Not Seen	626 (11.7)
The tobacco-free policy has reduced the use of tobacco and tobacco-derived products on the Columbia campus.	
Agree	3,621 (69.5)
Disagree	1,590 (30.5)
Observed tobacco products being smoked on campus property in past 30 days	
Yes	4,538 (93.5)
No	997 (6.5)
Number of days observed tobacco products being smoked on campus property in past 30 days	
1-2 days	844 (18.6)
3-5 days	894 (19.6)
6-9 days	661 (14.6)
10-19 days	628 (13.8)
20-29 days	251 (5.6)
Daily	1,260 (27.8)

Exposure to second hand smoke on campus from someone else's cigarette, cigar, pipe, or hookah in past 30 days	
Yes	3,779 (68.3)
No	1,756 (31.7)
Number of days were you exposed to second hand smoke on campus from someone else's cigarette, cigar, pipe, or hookah in past 30 days	
1-2 days	1,143 (30.2)
3-5 days	846 (22.4)
6-9 days	576 (15.2)
10-19 days	469 (12.4)
20-29 days	175 (4.6)
Daily	570 (15.1)
Observed smokeless tobacco use on campus property in past 30 days	
Yes	3,031 (54.8)
No	2,505 (45.2)
Number of days you observed smokeless tobacco use on campus property in past 30 days	
1-2 days	1,192 (39.3)
3-5 days	548 (18.1)
6-9 days	360 (11.9)
10-19 days	307 (10.1)
20-29 days	113 (3.7)
Daily	511 (16.9)
Observed electronic cigarette use on campus property in past 30 days	
Yes	3,241 (59.6)
No	2,200 (40.4)
Number of days you observed electronic cigarette use on campus property in past 30 days	
1-2 days	780 (24.1)
3-5 days	680 (21.0)
6-9 days	534 (16.5)
10-19 days	499 (15.4)
20-29 days	144 (4.4)
Daily	604(18.6)

Table 2. Selected Survey Results from the Healthy Carolina Survey, 2015
Notes: Number of responses varies per question and may not equal the full sample size. Proportions reported based on sample size for each respective question. Correct response indicated by asterisk.

	Accurate knowledge of policy, OR (95% CI)	Intervening on observed violations, OR (95% CI)	Positive opinion of policy effectiveness, OR (95% CI)
Status			
Undergraduate	**0.69 (0.57, 0.83)**	**0.45 (0.36, 0.56)**	**0.37 (0.30, 0.46)**
Graduate Student	**0.70 (0.58, 0.83)**	**0.31 (0.22, 0.43)**	**0.58 (0.44, 0.77)**
Faculty	**0.71 (0.55, 0.92)**	0.80 (0.58, 1.10)	**1.68 (1.16, 2.45)**
Staff	1.00	1.00	1.00
Gender			
Male	**0.81 (0.70, 0.94)**	**0.79 (0.66, 0.96)**	**0.48 (0.41, 0.56)**
Female	1.00	1.00	1.00
Race			
Non-white	0.85 (0.70, 1.03)	**1.28 (1.01, 1.61)**	0.90 (0.73, 1.12)
White	1.00	1.00	1.00

Table 3. Respondent Factors Associated with Selected Survey Outcomes
Note: Significant differences indicated in bold text with significance level defined at alpha=0.05.

DISCUSSION

The number of university campuses with tobacco-free policies continues to increase.[6] In addition, many members of university communities are aware of the hazards of second hand smoke and support a prominent role for the university in preventing smoke exposure through campus tobacco-free policies.[10-15,25] The effects of tobacco-free policies have generally been positive, including reduced smoking behavior,[8] and reduced second hand smoke exposure.[9] However, it is often unclear who should enforce such policies; when survey asked "If you did not approach the violator, please select the reasons why" 41% of survey respondents suggested that they did not believe they had the authority to address the issue.[13] This points towards a cited university student belief that campus police force or equivalent should be in charge of enforcing tobacco policies.[12,15]

The tobacco-free policy at USC puts the responsibility of enforcement on students, faculty, and staff. However, our results show many USC community members, particularly students and faculty, are not aware of the details of the current tobacco-free policy, nor do they feel comfortable with personally enforcing the policy. On the tobacco-free policy survey question 15 asked specifically, "What would make you feel more comfortable approaching a violator of the tobacco policy?" The most-often suggested solution offered by respondents was to increase tobacco-free signage on campus (N=2745). Signage is considered a passive way to address policy violations that can be ignored or vandalized. In our study, 17% of violations occurred within view of a tobacco-free or no-smoking sign. One alternative approach researchers suggested would include recruitment of "community enforcers" who have the authoritative power to address violators and issue citations. These community enforcers, who could include students, faculty or staff, would also receive special training on how to approach violators and educate them on the consequences of their behavior. There are currently tobacco-free ambassadors on the USC campus, but the training is on a volunteer basis, and awareness of the program is limited.[31] A more prominent community enforcement program on campus may

increase other community members' confidence in approach smoking violators and would not take campus police away from their existing community safety responsibilities. In a past study analyzing a tobacco ambassador program at another southeastern university, the use of a tobacco ambassador program (Tobacco Free Take Action!) reduced observed tobacco use by 65% and 35% reduction in cigarette butts found on campus hotspots.[33]

CONCLUSION

This project provided important information on the perceptions that university students and employees have regarding the campus tobacco-free policy. Tobacco use continues on campus, and many people (particularly students) do not intervene when observing violations of the policy, suggesting a need for interventions to improve confidence about approaching tobacco-free policy violators on campus. Additionally, many respondents did not know that e-cigarettes were included in the university's tobacco-free policy, indicating a need for Healthy Carolina and other administrative units to better educate student, faculty and staff about what types of products are not permitted on campus. Furthermore, university tobacco-free policies lacking clear consequences for violations and appropriate enforcement may not be sufficient in creating tobacco-free campus environments.

Limitations of this study include the inability to observe and pin observations of smokeless tobacco use on *Collector for ArcGIS*. Smokeless tobacco is often harder to observe and cannot be readily confirmed without directly approaching the violator. Additionally, we were unable to randomly assign times for volunteers to work. Because of their employment and class schedules, volunteers were asked to walk for 30 minutes to one hour whenever they were able to in a given week before 7PM (because of safety concerns). This eliminated tobacco-free violators from being observed during certain times of the day, such as early mornings, nights, and weekends.

ACKNOWLEDGEMENT

This work was supported in part by an undergraduate research award to S. Powell through the USC Office of Undergraduate Research. The funder did not design, implement, analyze, or interpret the results of the study.

REFERENCES

1. Bayer, R., Colgrove, J. (2002) Science, politics, and ideology in the campaign against environmental tobacco smoke. *Am J Public Health* 92(6), 949-954.
2. Chapman, S. (2007) *Health Advocacy and Tobacco Control: Making Smoking History*. Blackwell: Oxford.
3. World Health Organization. Protection from exposure to secondhand tobacco smoke: Policy recommendations. 2007; http://apps.who.int/iris/bitstream/10665/43677/1/9789241563413_eng.pdf (accessed July 2017)
4. Copeland, A., Peltier, M., and Waldo, K. (2017) Perceived risk and benefits of e-cigarette use among college students. *Addictive Behaviors* 71, 31-37.
5. Americans for Nonsmokers' Rights. Homepage. *http://www.no-smoke.org/* (accessed July 2017)
6. Americans for Nonsmokers' Rights. Going smokefree: colleges and universities. *http://no-smoke.org/goingsmokefree.php?id=447* (accessed May 2017)
7. Lee, J.G., Ranney, L.M., and Goldstein, A.O. (2013) Cigarette butts near building entrances: what is the impact of smoke-free college campus policies? *Tob Control* 22(2), 107-112.
8. Seo DC, Macy JT, Torabi MR, Middlestadt SE. (2011) The effect of a smoke-free campus policy on college students' smoking behaviors and attitudes. *Prev Med* 53(4-5), 347-352.
9. Lechner WV, Meier E, Miller MB, Weiner JL, Fils-Aime Y. (2012) Changes in smoking prevalence, attitudes, and beliefs over 4 years following a campus-wide anti-tobacco intervention. *J Am Coll Health* 60(7), 505-511.
10. Braverman, M.T., Hoogesteger, L.A., Johnson, J.A. (2015) Predictors of support among students, faculty and staff for a smoke-free university campus. *Prev Med* 71, 114-120.
11. Wallar LE, Croteau S, Estill A, Robson L, Papadopoulos A. (2013) Analyzing exposure, use, and policies related to tobacco use on campus for the development of comprehensive tobacco policies at Canadian post-secondary institutions. *J Community Health* 38(6), 1081-1089.
12. Burns S, Jancey J, Bowser N, Comfort J, Crawford G, Hallett J, Shields B, Portsmouth L. (2013) Moving forward: a cross sectional baseline study of staff and student attitudes towards a totally smoke free university campus. *BMC Public Health* 13, 738.
13. Marsh, L., Robertson, L.A., Cameron, C. (2014) Attitudes towards smokefree campus policies in New Zealand. *N Z Med J* 127(1393), 87-98.
14. Braverman MT, Hoogesteger LA, Johnson JA, Aaro LE. (2017) Supportive of a smoke-free campus but opposed to a 100% tobacco-free campus: identification of predictors among university students, faculty, and staff. *Prev Med* 94, 20-26.
15. Almutairi, K.M. (2014) Attitudes of students and employees towards the implementation of a totally smoke free university campus policy at King Saud University in Saudi Arabia: a cross sectional baseline study on smoking behavior following the implementation of policy. *J Community Health* 39(5), 894-900.

16. Baha, M., Le Faou, A.L. (2010) Smokers' reasons for quitting in an anti-smoking social context. *Public Health* 124(4), 225-231.
17. Rigotti, N.A., Moran, S.E., Wechsler, H. (2005) U.S. college students' exposure to tobacco promotions: prevalence and association with tobacco use. *Am J Public Health* 95(1), 138-144.
18. Ling, P.M., Neilands, T.B., Glantz, S.A. (2009) Young adult smoking behavior: a national survey. *Am J Prev Med* 36(5), 389-394.
19. Butler KM, Rayens MK, Hahn EJ, Adkins SM, Staten RR. (2012) Smoke-free policy and alcohol use among undergraduate college students. *Public Health Nurs* 29(3), 256-265.
20. Blanton, H., Köblitz, A., McCaul, K.D. (2008) Misperceptions about norm misperceptions: descriptive, injunctive, and affective 'social norming' efforts to change health behaviors. *Soc Personal Psychol Compass* 2(3), 1379-1399.
21. Stuber, J., Galea, S., Link, B.G. (2008) Smoking and the emergence of a stigmatized social status. *Soc Sci Med* 67(3), 420-430.
22. Ritchie, D., Amos, A., Martin, C. (2010) "But it just has that sort of feel about it, a leper"--stigma, smoke-free legislation and public health. *Nicotine Tob Res* 12(6), 622-629.
23. Stuber, J., Galea, S., Link, B.G. (2009) Stigma and smoking: the consequences of our good intentions. *Soc Serv Review* 83(4), 858-609.
24. Everett SA, Husten CG, Kann L, Warren CW, Sharp D, Crossett L. (1999) Smoking initiation and smoking patterns among US college students. *J Am Coll Health* 48(2), 55-60.
25. Rigotti NA, Regan S, Moran SE, Wechsler H. (2003) Students' opinion of tobacco control policies recommended for US colleges: a national survey. *Tob Control* 12(3), 251-256.
26. Harris KJ, Stearns JN, Kovach RG, Harrar SW. (2009) Enforcing an outdoor smoking ban on a college campus: effects of a multicomponent approach. *J Am Coll Health* 58(2), 121-126.
27. Lawrence D, Fagan P, Backinger CL, Gibson JT, Hartman A. (2007) Cigarette smoking patterns among young adults aged 18-24 years in the United States. *Nicotine Tob Res* 9(6), 687-697.
28. American College Association ACH. (2012) Position statement on tobacco on college and university campuses. *J Am Coll Health* 60(3), 266-267.
29. University of South Carolina. Tobacco free campus. http://www.sc.edu/policies/ppm/univ500.pdf. (accessed April 2016)
30. University of South Carolina. USC Columbia at a glance. http://southcarolina.edu/our_campuses/columbia.php. (accessed March 2017)
31. Healthy Carolina. Tobacco free USC. https://www.sa.sc.edu/healthycarolina/initiatives/tobacco/. (accessed April 2016).
32. University of South Carolina Student Health Services. Tobacco cessation - Student Health Services. https://www.sa.sc.edu/shs/cw/tobacco/. (accessed April 2016)
33. Ickes, M., Rayens, M.K., Wiggins, A.T., Hahn, E.J. (2015) A tobacco-free campus ambassador program and policy compliance. *Journal of American College Health* 63(2), 126-133.

ABOUT THE STUDENT AUTHOR

Sarah Powell completed this study in 2016 while she was an undergraduate public health student at the University of South Carolina (USC). She graduated cum laude from USC in May 2016 with a bachelor of science degree. Since graduating, she has enrolled at the University of South Florida College of Public Health to pursue her masters of science degree in epidemiology.

PRESS SUMMARY

With the large amount of college campuses creating tobacco-free policies that restrict or prohibit tobacco use there is interest in studying college communities' thoughts, opinions, and knowledge about the new policies. This study examined the tobacco-free policy at a large urban campus using an electronic survey that was sent to students, faculty, and staff. After analysis, the community demonstrated a tobacco-policy knowledge deficiency, and a lack of confidence in approaching people who continue to use tobacco. The research team at the conclusion of the study recommends an intervention on campus to increase tobacco-policy awareness and community confidence to approach violators of the policy.

Conduction Mechanism in Electrically Conducting Polymers

*Daniel L. Gochnauer & T. H. Gilani**

Department of Physics, Millersville University, P. O. Box 1002, Millersville PA-17551

Student: dlg15@uw.edu
Mentor: tariq.gilani@millersville.edu

ABSTRACT
The conduction mechanism in conducting polymers is reviewed and experimental results of temperature dependence of electrical conductivity of PF_6 doped polypyrrole in temperature range of 77 to 300 K are discussed. The room-temperature conductivity was experimentally determined to be 73 ± 3.4 S/m and temperature dependence follows the Mott's variable range hopping model. The average hopping distance at 298 K was (6.75 ± 0.97) $\times 10^{-8}$ cm. The coefficient of decay of the localized states, the density states at the Fermi level, and the hopping activation energy were calculated to be (3.5±0.51) $\times 10^{7}$ cm^{-1}, (1.92 ± 0.83) $\times 10^{22}$ cm^{-3} eV^{-1}, and 0.040 ± 0.001 eV respectively.

KEYWORDS:
Electrically Conducting Polymers; Doped Polypyrrole; Temperature Dependence of Conductivity; Hopping Activation Energy; Density of State at Fermi Level

INTRODUCTION

The study of electrically conducting polymers, with its many potential applications, deserves recognition as an important frontier in materials science research and development.[1-2] These conducting polymers have many potential applications. At present they are used as antistatic materials, transparent conductive layers, and protective finishes in printed circuits. Additionally, an increasing focus on organic light emitting diodes and organic polymer solar cells show yet another trend for their future applications.[1]

The electrically conducting polymers have been synthesized with conductivities as high as 10^3 or 10^4 $S \cdot cm^{-1}$,which is merely 1 or 2 orders of magnitude less than that of metals.[3-4] The conductivity of doped polypyrrole (PPy) can be as high as 10^4 $S.cm^{-1}$. In addition, the higher stability and durability of PPy, makes it an excellent candidate for study.[2]

PPy doped with hexafluorophosphate (PF_6), hereafter called PPy (PF_6), was synthesized and its electrical resistivity was experimentally measured as a function of temperature. The purpose of the study was to develop a better understanding of the conduction mechanism in PPy (PF_6).

In metals, the number of valence electrons is minimal compared to the number of available energy orbitals, resulting in higher degrees of freedom allowing the electrons to be delocalized. This enables the electrons to change energy levels within a metal atom, as well as move into the available orbitals in neighboring atoms. In an environment with zero applied electric field, electrons are still moving across the metal surface, but with no net displacement. When an electric field is applied, the electrons still move in random directions, but now there will is a net bias of movement in the direction of the applied electric field.[5]

The same conditions for conductivity are also required in the electrically conducting polymers: delocalized charged carriers and partially filled energy bands. In most organic molecules, however, the valence electrons are localized, due to their participation in the intra-molecular bonds between the atoms. Additionally, due to the covalent nature of nonmetallic bonds, atoms in organic molecules tend not to have the high number of available energy orbitals that metals demonstrate as shown in **Figure 1**. The solution to this problem lies in the use of conjugated double bonds. A conjugated double bond exists when an organic molecule has alternating single and double bonds, where single and double bonds are defined as chemical bonds between two atoms involving one or two pairs of shared electrons, respectively. The simplest example of a system of conjugated double bonds is trans-polyacetylene, which is also an electrically conductive polymer.

It is the second pair of electrons in the double bonds, which becomes delocalized. One pair of electrons, which holds two atoms together, is denoted as the σ-bond; any additional pairs are denoted as π-bonds, which are not required to maintain the bond structure. The σ-bonds are formed by the two atoms' overlapping s-orbitals and pz-orbitals, parallel to the axis of the bond. The π-bonds are typically formed by a sharing of electrons between the p_x- and p_y-orbitals, which are perpendicular to the axis of the bond.[6] For a system with only one double bond, there would be no available orbitals in the adjacent atoms, and so the double bond would be localized. In trans-polyacetylene, however, all of the atoms in the chain have partially filled π- bonding p-orbitals available.

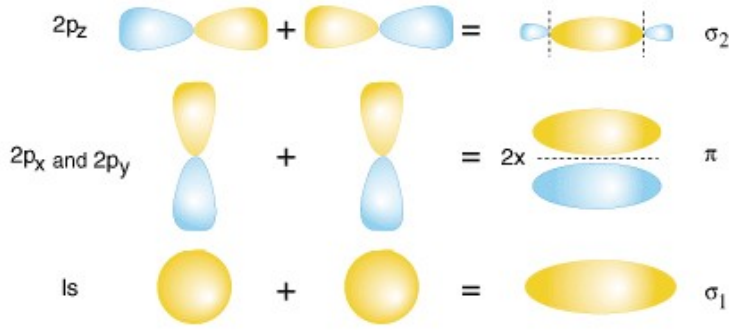

Figure 1. The molecular bonding orbitals for the 1s, $2p_z$, $2p_x$ and $2p_y$ orbitals. The 1s and $2p_z$ orbitals contribute to the single bonding.[6]

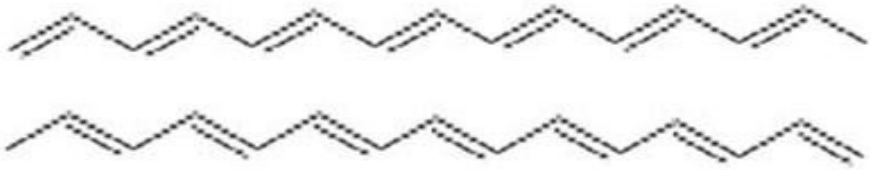

Figure 2. The two forms of trans-polyacetylene are energetically degenerate. In this diagram, each vertex represents a carbon atom, each line represents a bonding pair of electrons, and all of the hydrogen atoms are omitted, as is conventional.[7]

Charge Carriers in Polymers

Another way to consider this system is as a chain of singly bonded carbons, each with one spare valence electron. Any two adjacent atoms can then share their lone electron to form a double bond; therefore, the energy of such systems as shown in **Figure 2** would be lowest. This concept can be extended to the idea that these conjugated, or delocalized, double bonds are able to transport charges effectively within the system. Indeed, such a mechanism for this phenomenon had already been proposed[8] that charge can be carried by quasi-particles such as solitons, polarons, and bipolarons. A soliton is formed when the chain of double bonds is in a state where there is a single atom, which is not sharing its electron with either of its neighboring atoms. In this state, one of the adjacent atoms can change from its state of π-bonding with the tertiary atom to a state of π-bonding with the primary atom in question. These two states are also degenerate, with each other as well as with the states. Thus, this process can occur both naturally and spontaneously. A soliton can become delocalized and is considered to be the most basic charged carrier in conjugated double bond systems.[6]

In other words, it is not likely that a particular electron is moving across the chain of atoms, but rather, it is simply the order of pairing combinations in the polymer, which changes, allowing the soliton to carry the charge along the chain. This is why the soliton, and related particles, such as the polaron and bipolaron are often referred to as quasi- particles. A soliton is like a fermion in that it has a quantum spin value of ±½; however, it differs from the traditional charge carrier, electrons, in that it has zero charge.

A polaron is another type of charged carrier in conjugated double bond polymers with spin ±½. Unlike the soliton, however, the polaron has an electric charge of ± *e*. In many of these types of polymers, it is a common practice to dope the polymer with positively or negatively charged ions in order to make it more electrically conducting. Here, "dopant" is used to mean a chemical additive, which may change the properties of the polymer, as opposed to the more common use of the word in semiconductor physics. When the polymer is doped with negative ions, as is most common, some of the carbon atoms on the chain obtain a positive formal charge.[1] This alteration to the system allows for an additional mechanism for charge transportation; the traditional electron "hole" may transport charge along the polymer chain. The polaron, then, exists as a coupling of this positive charge with the unpaired electron from a soliton.[9] Unlike a soliton, however, the polaron has a certain length, given by the distance between the coupled electron and hole. This distance decreases as the concentration of dopant anions increases. Also, as expected, the number of polarons continues to increase as more ions are added.

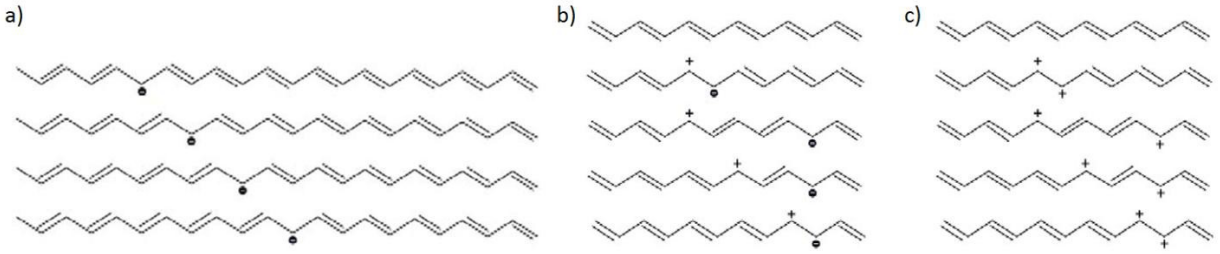

Figure 3. (a) Formation of a soliton in trans-polyacetylene retains the same energetic degeneracy as before. Charge is transported as the soliton hops along the carbon chain.
(b) This diagram shows a mechanism for transportation of a polaron along trans-polyacetylene. The length of the polaron is allowed to vary, as the lone electron and the hole move independently.
(c) The mechanism for bipolaron transportation is analogous to polaron transportation.

Note that in both pictures, however, the counter ions are not shown; they cannot be designated to a specific carbon atom because the positive charge is delocalized.[7]

When the concentration of counter ions increases past a certain point, two polarons may then couple to form another quasi-particle called a bipolaron.[8,9] Like polarons, bipolarons have a certain length; this length is now defined by the distance between two of the positively charged atoms. Compared to the soliton and the polaron, the bipolaron is unique in that it is a bosonic particle with quantum spin values of 0 or 1 but a bipolaron will have a charge of $\pm 2e$. The formations of a soliton, a polaron and a bipolaron are depicted in **Figure 3**.

Band Gap Theory

The conductive effects of solitons, polarons, and bipolarons can be described effectively using band gap theory. In terms of energy band gap regimes, undoped electrically conducting polymers can be thought of as semiconductors. Therefore, the energy gap between the valence and the conduction band is relatively small, and certain means may be used to allow valence electrons to become excited up into the conduction band. The process of direct ionization requires that an electron must have at least enough energy to jump from the highest occupied energy level to the lowest unoccupied energy level, with no assistance.[10] In a polaron, however, the lowest unoccupied energy level is increased and the highest occupied energy level decreases, by a value corresponding to the polaron's binding energy. Additionally, the energy gap for a bipolaron is decreased even further, by an amount corresponding to the coupling energy of two polarons. The situations are presented in **Figure 4** and **Figure 5**.

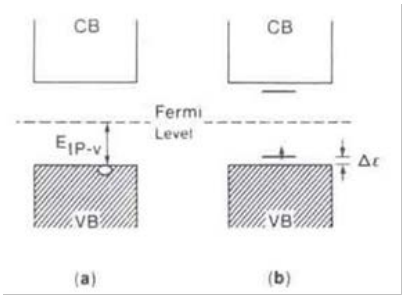

Here, the reference level is the Fermi level, E_{IP-V} is half the energy required for the ionization process, and $\Delta\varepsilon$ corresponds to the binding energy of the polaron.[10]

Figure 4. This image compares the energy band gaps for an electrically conductive polymer (a) with no polaron and (b) with a polaron.

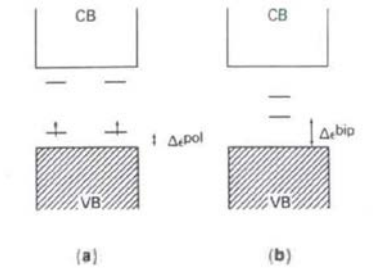

Here, $\Delta\varepsilon^{pol}$ represents the binding energy of a polaron and $\Delta\varepsilon^{bip}$ represents the combined binding energy as well as the coupling energy of the two polarons.[10]

Figure 5. Two polarons would have the same decrease in energy band gap. However, the coupling of two polarons would effectively decrease the gap further.

This concept can be extended to the idea that polymer conductivity may be dependent on dopant concentration. Dopant concentration is directly related to the number of positively charged atoms along the chain, and therefore the concentration of polarons. Subsequently, with increasing numbers of polarons, there will be more polarons coupling to form bipolarons. For incredibly highly doped polymers, the bipolaron's energy levels spread out into new energy bands, in the same way that traditional atomic energy levels form the conduction and valence energy bands.[10] This results in a minimum energy gap. These energy bands between the original conduction and valence bands allow for a greater population of electrons to carry charge via this new array of available energy levels. This whole process shows how doping electrically conductive polymers can lead to a decreased energy band gap for electronic excitation, which aids in increasing the conductivity of the material.

Variable Range Hopping Model

Several models[11] have been proposed to describe the conduction mechanisms in conducting polymers. One of the models that describes quantitatively the transportation of charge within the conducting polymers is Mott's variable range hopping model.[12] This model assumes that the charge hops along the polymer chain in the form of a soliton as previously discussed, unlike an electron does in a pure metal conductor. Mott's variable range hopping model relates the conductivity σ with the temperature, T by the following equation:

$$\ln \sigma = \ln \sigma_0 - \left({}^{T_0}/_{T}\right)^{\frac{1}{4}} \qquad \textbf{Equation 1.}$$

The characteristic conductivity, σ_0 and the characteristic temperature, T_0 can be easily obtained from the temperature dependence of the electrical conductivity, σ. These variables are related to other key parameters by the following additional equations:

$$\sigma_0 = e^2 R^2 v_{ph} N(E_F) \qquad \textbf{Equation 2.}$$

$$T_0 = \frac{\lambda\, \alpha^3}{k\, N(E_F)} \qquad \textbf{Equation 3.}$$

$$R = \left(\frac{9}{8\pi\alpha k T N(E_F)}\right)^{\frac{1}{4}} \qquad \textbf{Equation 4.}$$

$$W = \frac{3}{4\pi R^3 N(E_F)} \qquad \textbf{Equation 5.}$$

In above equations, e is the charge of an electron (1.602×10^{-19} C), k is the Boltzmann constant (8.616×10^{-5} eV K^{-1}), v_{ph} is the phonon frequency, λ is a dimensional constant, a is coefficient of decay of the localized states, R is the average hopping distance, $N(E_F)$ is the density of localized states at the Fermi level, and W is the hopping activation energy.

Values of σ_0 and T_0 can be found by fitting the experimental data of temperature dependence of conductivity to the model given in **Equation 1**. Then fixing ν_{ph} and λ, the values of other four unknown variables R, N, W, and a can be obtained algebraically from four equations, **Equation 2** through **Equation 5**. This could be done by hand, but we have tools like Mathematica to do it faster.

EXPERIMENT AND RESULTS

Incidentally, the process of synthesizing and doping polypyrrole can be carried out in a single reaction. The reaction of pyrrole monomers to form the polymer, polypyrrole is an oxidation reaction, and because that product needs further oxidized for the addition of negatively charged dopants, it is convenient to carry out both reactions in a single electrochemical cell. The reaction is carried out in a an electrochemical cell, consisting of a simple glass beaker, containing a specially prepared solution at 25 °C for the reaction[3, 4, 13] and using a platinum coated anode (approximately 25 mm x 75 mm x 1 mm). The prepared solution contained 0.288 M pyrrole monomer, 0.054 M KPF_6, and 0.123 M $FeCl_3$ dissolved in distilled water. Here, $FeCl_3$ was used as an oxidizing agent. During the synthesis, 4.2 ± 0.8 V were applied across the electrodes for 1 to 2 hours,[14] after which the polymer film is removed from the anode and left to dry at room temperature for another 24 hours. The polymerization process can be represented schematically in **Figure 6 (a) and 6 (b)**.

Various samples were obtained and the best of them were used for the measurements. Typical sample size was 15±1 mm × 3.5±0.5 mm × 0.010±0.005 mm. The four-probe method was used to measure resistance at atmospheric pressure while varying the temperature from 77 K to 300 K. The schematic diagram of the four-probe method is shown in **Figure 6 (c)**.

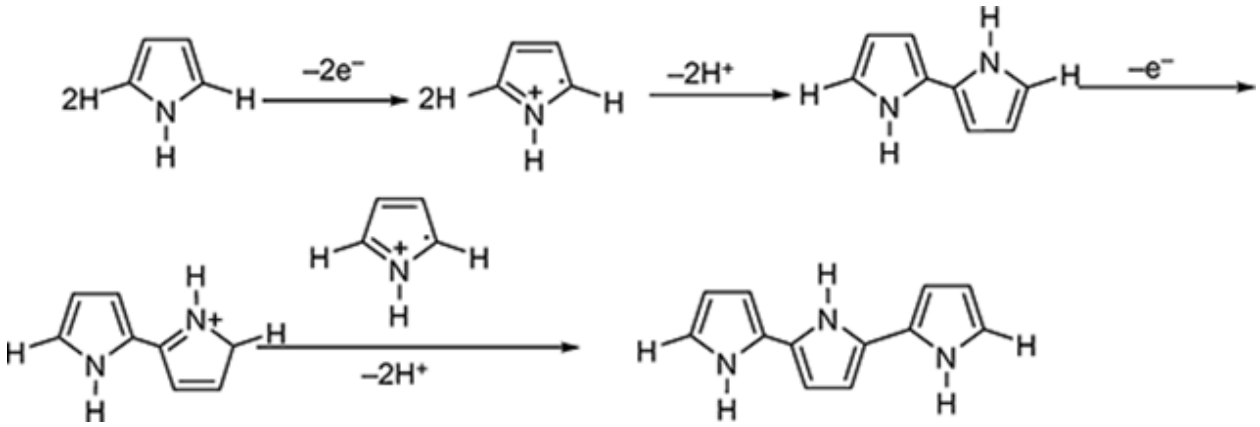

Figure 6 (a) Polymerization of polypyrrole.

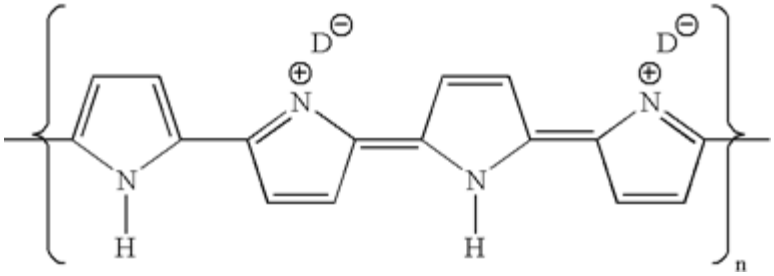

Figure 6 (b) Schematics of doped polypyrrole with an arbitrary dopant ion D.

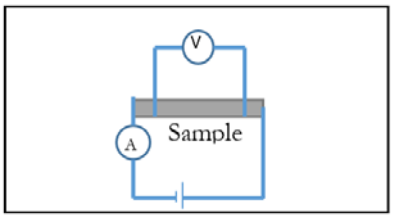

Figure 6 (c) Schematic diagram of the four-probe method for resistance measurement.

The room temperature resistance measurements show Ohmic behavior of the sample at low voltage and current range as shown in **Figure 7**. The electrical conductivity at room temperature (298 K) and atmospheric pressure was 73 ± 3.4 S/m, obtained from the graph shown in **Figure 7**.

The temperature dependence of electrical conductivity is shown in **Figure 8**, where $\ln(\sigma)$ is plotted versus $T^{-1/4}$. A straight line is obtained as suggested by Mott's variable range hopping model.[12] The corresponding equations (**Equation 2** to **Equation 5**) were used to determine the values of the average hopping distance, *R*, the density of localized states at the Fermi level, $N(E_F)$, and the hopping activation energy, *W*, and the coefficient of decay of the localized states, *a*. Note that the temperature of liquid nitrogen, 77 K, was not actually achieved; this was simply because the sample was not directly in contact with the nitrogen, and so the system could not cool all the way to 77 K.

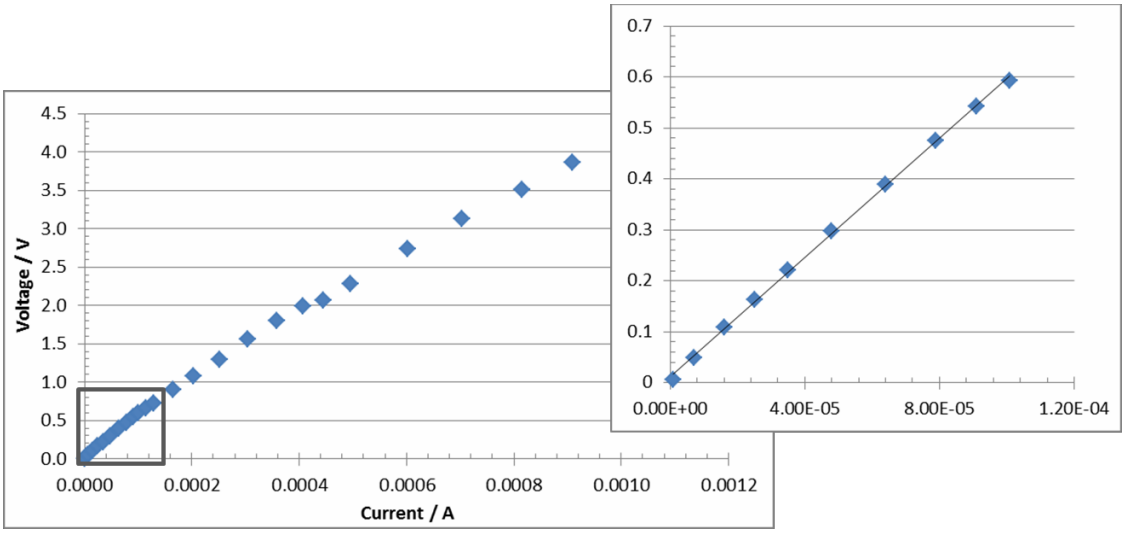

Figure 7. Voltage vs current behavior of PF_6^- doped polypyrrole at room temperature. The region in the square is enlarged and clearly shows Ohmic behavior.

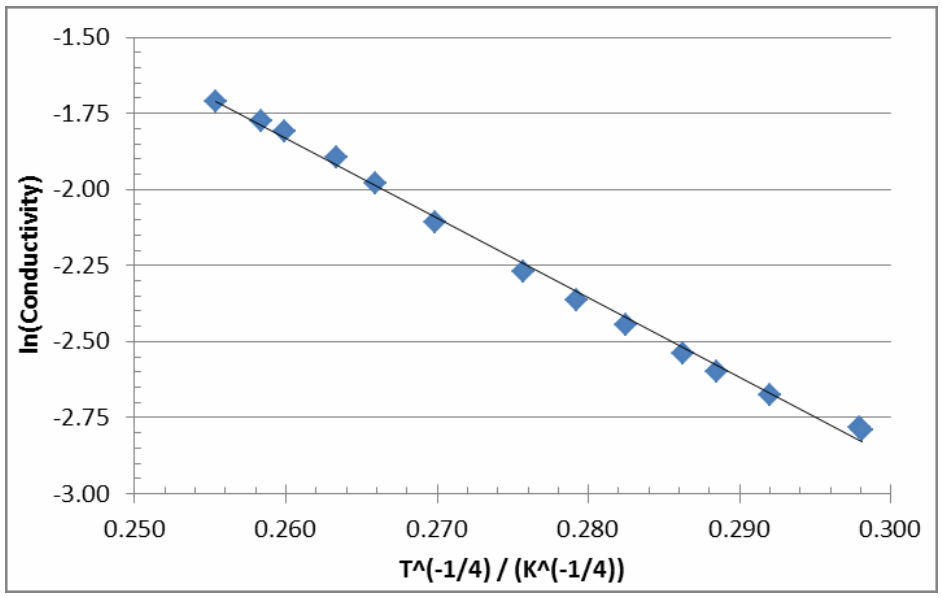

Figure 8. Temperature dependence of conductivity of PF_6^- doped Polypyrrole, which fits Mott's variable range hopping model given in Equation 1.

DISCUSSIONS

From **Figure 8**, along with **Equation 1**, the characteristic conductivity, σ_0, and the characteristic temperature, T_0, were determined to be 140 ± 20 S/cm and (4.7 ± 0.3) × 10^5 K, respectively. The values were subsequently used along with **Equation 2** through **Equation 5** to determine the values of the average hopping distance, R, the density of localized states at the Fermi level, $N(E_F)$, and the hopping activation energy, W. The phonon frequency, ν_{ph}, was set to be 10^{13} Hz and the dimensional constant, λ, was set to be 18.1.[12]

Expressed in terms of the known parameters and the returned fit parameters, the expressions for R, N, W, and a (given in **Equation 2** through **Equation 5**) can also be re-written as following:

$$R = \frac{3\sqrt{3}e^2\nu_{ph}\,\lambda^{1/4}}{4\times 2^{1/4}k\,\pi^{3/4}T^{3/4}{T_0}^{1/4}\sigma_0} \qquad \textbf{Equation 6.}$$

$$N = \frac{16\sqrt{2}\,k^2\pi^{3/2}T^{3/2}\sqrt{T_0}\,{\sigma_0}^3}{27e^6{\nu_{ph}}^3\sqrt{\lambda}} \qquad \textbf{Equation 7.}$$

$$\alpha = \frac{2k\sqrt{2\pi}\sqrt{T}\sqrt{T_0}\sigma_0}{3e^2\nu_{ph}\sqrt{\lambda}} \qquad \textbf{Equation 8.}$$

$$W = \frac{k\left(\frac{2}{\pi}\right)^{1/4} T^{3/4} T_0{}^{1/4}}{\sqrt{3}\,\lambda^{1/4}}$$ **Equation 9.**

We start with the assumption that the solitons are the primary charged carriers in conducting polymers. The average hopping distance *R*, the density of states at the Fermi level $N(E_F)$, the hopping activation energy *W,* and the coefficient of decay of the localized states *a* were then calculated and following values were obtained at 298 K temperature:

$R = (6.75 \pm 0.97) \times 10^{-8}$ cm
$N(E_F) = (1.92 \pm 0.83) \times 10^{22}$ cm^{-3} eV^{-1}
$W = 0.041 \pm 0.001$ eV
And $a = (3.50 \pm 0.51) \times 10^{7}$ cm^{-1}

The mechanism of charge transportation in doped polypyrrole follows the pattern of Mott's variable range hopping model, supported by the experimental data shown in **Figure 8**. Additionally, the data shows that conductivity increases as temperature increases. This is the behavior of a typical semiconductor, which can be explained by Band gap theory. The values of the calculated parameters all fall within the same order of magnitude when compared with the corresponding values calculated in References 12 and 15. Although these references represent different polymers and dopants, it shows that the results of this experiment fall in the same range. These references view the conduction mechanism in electrically conducting polymers as charge being carried by polarons and the parameters have been calculated based on doped-polyacetylene while the charged carriers in doped PPy are thought to be bipolarons.[9] However, it is not clear if a bipolaron hops itself or if it breaks into two polarons before hopping. Two polarons can then recombine to form a bipolaron after hoping. Since we obtained parameters, especially average hopping distance, in the same range as calculated for polarons in references 12 and 15, we can conclude based on experimental results that the charged carriers in doped-PPy are polarons with the average hopping distance of approximately $(6.75 \pm 0.97) \times 10^{-8}$ cm. We must note that the parameter values obtained here are based upon studies on polypyrrole, while polyacetylene is another class of electrically conducting polymers. However, polyacetylene and polypyrrole have very different backbone structure.

ACKNOWLEDGEMENT
This project was supported by funding from the Millersville University Physics Department as well as the Millersville Student Research Grant Program. Necessary facilities and equipment have also been made available through Millersville University. Additionally, the assistance provided by Mr. Shawn Reinfried has been most helpful. The platinum electrode was generously supplied by Mark Geusic, President of Optimum Anode Technologies.

REFERENCES

1. Walton, D. (1990) Electrically Conducting Polymers, *Materials and Design*, 11, 142-152.
2. Skotheim, T. A., Elsenbaumer, R. L., Reynolds, J. R. (1998) *Handbook of Conducting Polymers*, Eds., 2nd Ed., Marcel Dekker, New York and references there in.
3. Yamaura, M., Hagiwara, T., Iwata, K. (1988**)** Synth. Met. 26**,** 209-212.
4. Hagiwara, T., Hirasaki, M., Sato, K., Yamaura, M. (1990**)** *Synth. Met.* 36, 241-246.
5. See, for example, Stephen Elliott (2000) The Physics and Chemistry of Solids, Wiley
6. SparkNotes: *Molecular Orbital Theory*
   http://www.sparknotes.com/chemistry/bonding/molecularorbital/section1.rhtml Accessed on Feb. 2014
7. Nordén, B. (2000, October 12) *Conductive Polymers - a Surprising Discovery*
   http://www.surfacefinishing.com/doc/conductive-polymers-a-surprising-discovery-0001 Accessed on Feb. 2014
8. Gilani, T. (Dec.16-18, 1997) Transport Properties of dopedPolypyrrole, *Frontiers in Physics, Proceeding of 6th National Symposium on Frontiers in Physics, Quaid-i-Azam Univ., Islamabad, Pakistan*, 123-130.
9. Gilani, T., Ishiguro, T. (1996) Low-temperature metallic conductance in PF_6-doped Polypyrrole, *Synth. Metals*, 78, 327-331.
10. Brédas, J. and Street, G. (1985) Polarons, bipolarons, and solitons in conducting polymers, *Acc. Chem. Res.*, 18, 309-315.
11. Gilani, T. (2005) Evidence for Metal-like Electronic Contribution in Low-temperature Heat Capacity of Polypyrrole, *J. Phys. Chem. B*, 109, 19204 and reference there in.
12. Kaynak, A. (1998) DC Conduction in Electrochemically Synthesized Polypyrrole Films, *Tr. J. Chemistry*, 22, 81-85.
13. Chitte, H., Bhat, N., Walunj, V. and Shinde, G. (2011) Synthesis of Polypyrrole using Ferric Chloride ($FeCl_3$) as oxidant together with some dopants for use in gas sensors, *J. Sensor Technology*, 1, 47-56.
14. Shoa, T., Cole, M., Munce, N., Yang, V. and Madden, J. (2007) Polypyrrole operating voltage limits in aqueous sodium hexafluorophosphate, *Proc. SPIE*, 6524, 6524211-6524218.
15. Vernitskaya, T. and Efimov, O. (1997) Polypyrrole: a conducting polymer; its synthesis, properties and applications, *Rus. Chem. Rev.*, 66, 443-457.

ABOUT THE STUDENT AUTHOR

Daniel Gochnauer graduated from Millersville University, PA in 2014 with B. Sc. in Physics and Chemistry, and is now a graduate student at the University of Washington.

PRESS SSUMMARY

The development of electrically conducting polymers maintains its worth as a valued field of materials science and solid state physics. The focus in this article is conduction mechanism in electrically conducting polymers. A short-review of the conduction mechanism is presented. Also experimental results of temperature dependence of electrical conductivity of PF_6 doped polypyrrole in temperature range of 77 to 300 K are discussed in reference with Mott's variable range hopping model. The temperature dependence of conductivity follows the Mott's model. The average hopping distance, the density states at Fermi level and the hopping activation energy were determined from the experimental data.

Print Edition ISSN 1536-4585
Online Edition ISSN 2375-8732